

2014 年度

博士論文

Highly Sensitive Compositional Analysis of Biodegradable Copolyesters by
Reactive Pyrolysis-Gas Chromatography

反応熱分解ガスクロマトグラフィーによる
生分解性コポリエステルにおける共重合組成の高感度解析

Chubu University, Japan

Department of Biological Chemistry

Graduate School of Bioscience and Biotechnology

Siti Baidurah

A dissertation submitted to the Chubu University
in partial fulfillment for
the degree of Doctor of Philosophy
at Graduate School of Bioscience and Biotechnology

Siti Baidurah

2015

Contents

Chapter 1

Background and Aim of this Study

1.1	Definition and Classification of Biodegradable Polymers	2
1.2	Importance of the Compositional Analysis of Biodegradable Copolyesters	13
1.3	Compositional Analysis of Copolymers by Reactive Pyrolysis-Gas Chromatography (Reactive Py-GC)	20
1.3.1	Pyrolysis-Gas Chromatography (Py-GC)	20
1.3.2	Reactive Pyrolysis-Gas Chromatography (Reactive Py-GC)	21
1.4	Objectives of the Present Research	28

Chapter 2

Evaluation of Biodegradability of Poly(Butylene succinate-co-butylene adipate) on the Basis of Copolymer Composition Determined by Reactive Pyrolysis-Gas

Chromatography

2.1	Introduction	32
2.2	Experimental	34
2.2.1	Materials	34
2.2.2	Soil Burial Biodegradation Test	34
2.2.3	Reactive Py-GC Measurement	37
2.2.4	¹ H-NMR measurement	37

2.3	Results and Discussion	40
2.3.1	Compositional Analysis of the P(BS- <i>co</i> -BA) Samples	40
2.3.2	Reactive Py-GC of P(BS- <i>co</i> -BA) Samples after Soil Burial Degradation Test	47
2.3.3	Local Biodegradation in P(BS- <i>co</i> -BA) Film Samples Evaluated by Reactive Py-GC	51
2.4	Conclusions	53
	References	54

Chapter 3

Evaluation of Biodegradation Behavior of Poly(butylene succinate-*co*-butylene adipate) with Lowered Crystallinity by Reactive Pyrolysis-Gas Chromatography

3.1	Introduction	56
3.2	Experimental	59
3.2.1	Materials	59
3.2.2	Soil Burial Biodegradation Test	59
3.2.3	Differential Scanning Calorimetry (DSC) measurement	60
3.2.4	Reactive Py-GC Measurement	60
3.3	Results and Discussion	61
3.4	Conclusions	68
	References	69

Chapter 4

Rapid and Direct Compositional Analysis of Poly(3-hydroxybutyrate-co-3-hydroxyvalerate) in Whole Bacterial Cells by Reactive Pyrolysis-Gas

Chromatography

4.1	Introduction	71
4.2	Experimental	74
4.2.1	Materials	74
4.2.2	Culture conditions of <i>C. necator</i> for P(3HB-co-3HV) copolymer production	74
4.2.3	Reactive Py-GC measurement	77
4.2.4	Procedure for trans-methylation and solvent extraction followed by GC analysis	77
4.3	Results and Discussion	79
4.4	Conclusions	89
	References	90

Chapter 5

Conclusion and Future Prospects	93
--	----

List of Publication	95
----------------------------	----

Acknowledgements	96
-------------------------	----

Chapter 1

Background and Aim of this Study

1.1 Definition and Classification of Biodegradable Polymers

Biodegradable polymers undergo decomposition into water and carbon dioxide by various environmental microorganisms, such as bacteria and fungi.^{1,2} Figure 1.1 shows their biodegradation mechanism.¹ The decomposition starts on the polymer surface by the action of extracellular enzymes of microorganisms, generating oligomers. These oligomers enter the microorganism cell, in which they act as carbon sources and are completely metabolized into water and carbon dioxide.¹ Biodegradable polymers have attracted a great deal of attention as “green” polymeric materials because of their low environmental load upon disposal.

Table 1.1 shows the classification of typical commercially available biodegradable polymers based on their origins, with their trade names and manufacturers.³ These polymers generally consist of polyesters and polysaccharides bearing hydrolyzable ester or ether bonds in their backbones, respectively. They can be categorized according to their origins, namely bacteria, natural products, and chemical synthesis.³ In our present study, we briefly describe some polymers in these three groups by focusing on their properties and applications.

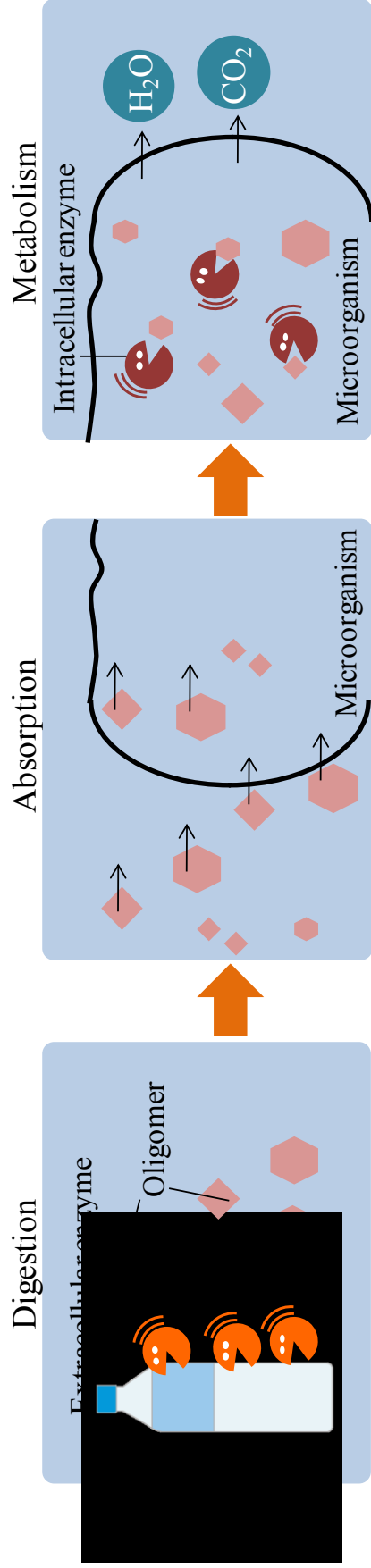
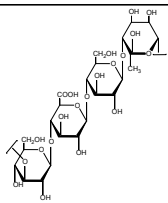
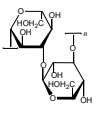
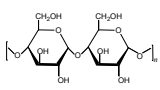
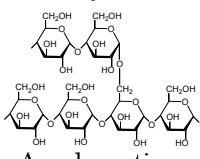
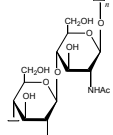
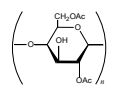


Figure 1.1 : Biodegradation mechanism of biodegradable polymers.¹

Table 1.1 : Classification of typical commercially available biodegradable polymers based on their origins and with their manufacturers.³

Origin : I. Biodegradable polymers produced by bacteria	
Polymer name and chemical structure	Trade name, Manufacture
$\left(-O-\underset{\text{CH}_3}{\text{CH}}-\text{CH}_2-\overset{\text{O}}{\parallel}{\text{C}}- \right)_n$ <p>Polyhydroxybutyrate (PHB)</p>	Biopol™, Monsanto Company Imperial Chemical Industries
$\left(-O-\underset{\text{CH}_3}{\text{CH}}-\text{CH}_2-\overset{\text{O}}{\parallel}{\text{C}}-\right)_x / \left(-O-\underset{\text{C}_2\text{H}_5}{\text{CH}}-\text{CH}_2-\overset{\text{O}}{\parallel}{\text{C}}-\right)_y \right)_n$ <p>Polyhydroxybutyrate-co-hydroxyvalerate (PHB-co-HV)</p>	
 <p>Gellan gum</p>	Kelcogel [®] , Kelco Biopolymers
 <p>Curdlan</p>	Pureglucan [®] , Takeda Chemical Industries (Japan) Nurture, Inc. (USA)
Origin : II. Biodegradable polymers produced from natural products and their derivatives	
 <p>Amylose</p>	Mater-Bi [®] , Novamont (Europe) Vegemat [®] , Vivadur (French)
 <p>Amylopectine Starch</p>	
 <p>Chitin</p>	Eastman Chemical Company (USA) Primester (USA) Celanese Ltd. (USA)
 <p>Cellulose acetate (CA)</p>	ChitoPure [®] , USA Biopolymer Engineering (US)

Origin : III. Biodegradable polymers produced via chemical synthesis

Polymer name and chemical structure	Trade name, Manufacture
$\left(\begin{array}{c} \text{O} \quad \text{O} \quad \text{R} \\ \parallel \quad \parallel \quad \\ \text{---} \text{C} \text{---} \text{C} \text{---} \text{O} \text{---} \text{C} \text{---} \text{C} \text{---} \text{O} \text{---} \\ \quad \quad \\ \text{R} \quad \text{R} \quad \text{R} \end{array} \right)_n$ <p>Polyglycolic Acid (PGA)</p>	Biomax ^R , Dupont
$\left(\begin{array}{c} \text{CH}_3 \quad \text{O} \\ \quad \parallel \\ \text{---O---CH}_2\text{---C---} \\ \\ \text{---} \end{array} \right)_n$ <p>Poly(lactic acid) (PLA)</p>	Mitsui Toatsu Chemical (Japan) NatureWorks TM , Cargill Dow (USA)
$\left(\begin{array}{c} \text{O} \\ \parallel \\ \text{---O---(CH}_2\text{)}_5\text{---C---} \\ \\ \text{---} \end{array} \right)_n$ <p>Polycaprolactone (PCL)</p>	Capa ^R , Solvay Group
$\left(\begin{array}{c} \text{O} \quad \text{O} \\ \parallel \quad \parallel \\ \text{---O---(CH}_2\text{)}_4\text{---O---C---(CH}_2\text{)}_2\text{---C---} \\ \quad \\ \text{---} \quad \text{---} \end{array} \right)_n$ <p>Poly(butylene succinate) (PBS)</p>	Bionolle, Showa Highpolymer (Japan)
$\left(\begin{array}{c} \text{O} \quad \text{O} \quad \text{O} \quad \text{O} \\ \parallel \quad \parallel \quad \parallel \quad \parallel \\ \text{---O---(CH}_2\text{)}_4\text{---O---C---(CH}_2\text{)}_2\text{---C---/---O---(CH}_2\text{)}_4\text{---O---C---(CH}_2\text{)}_4\text{---C---} \\ \quad \quad \quad \\ \text{---} \quad \text{---} \quad \text{---} \quad \text{---} \end{array} \right)_n$ <p>Poly(butylene succinate-<i>co</i>-butylene adipate) P(BS-<i>co</i>-BA)</p>	

I. Biodegradable polymers produced by bacteria

Some polyesters and polysaccharides accumulate in bacteria as intracellular carbon and energy compounds.^{3,4} Polyhydroxyalkanoates (PHAs) are biodegradable aliphatic polyesters formed entirely by bacterial fermentation. PHAs exist in over 90 bacteria genera.⁵ *Alcaligenes eutrophus* has been extensively studied because of its ability to produce large amounts of poly(3-hydroxybutyrate) (PHB).⁴ PHB accumulation in *A. eutrophus* can be controlled by changing the types or concentrations of carbon and nitrogen sources.^{4,6} For example, *A. eutrophus* produced PHB up to 80% of the dry weight when grown in a medium containing an excess of carbon sources, such as glucose, compared to nitrogen sources.^{4,7} PHB is synthesized in bacterial cells from acetyl coenzyme (CoA) by the sequential action of three enzymes (Figure 1.2). The first enzyme, 3-ketothiolase, catalyzes the reversible condensation of two acetyl-CoA moieties into acetoacetyl-CoA. Acetoacetyl-CoA is subsequently reduced by Acetoacetyl-CoA reductase into R-(-)-3hydroxybutyryl-CoA, which is polymerized into PHB by the action of PHA synthase.⁵

In general, the brittleness of PHB, caused by its high crystallinity, has limited its use as a material.⁸⁻⁹ To improve its toughness and flexibility, various comonomers, such as 3-hydroxyvalerate (3HV) units, are often introduced into the polymer chains by bacterial fermentation. The resulting copolymer poly(3-hydroxybutyrate-*co*-3-hydroxyvalerate) (P(3HB-*co*-3HV)) is currently used in internal sutures in the biomedical industry because of its high biocompatibility and nontoxicity.^{10,11}

Gellan gum and curdlan are biodegradable polysaccharides produced by bacteria.^{3,12-14} They have mainly been utilized as food additives, especially gelling and

thickening agents, because of their high water absorbency and nontoxicity.^{3,12-14} Edible films using gellan gum and curdlan have recently been developed and are expected to find application as food wrapping because of their high water vapor permeability.¹⁵

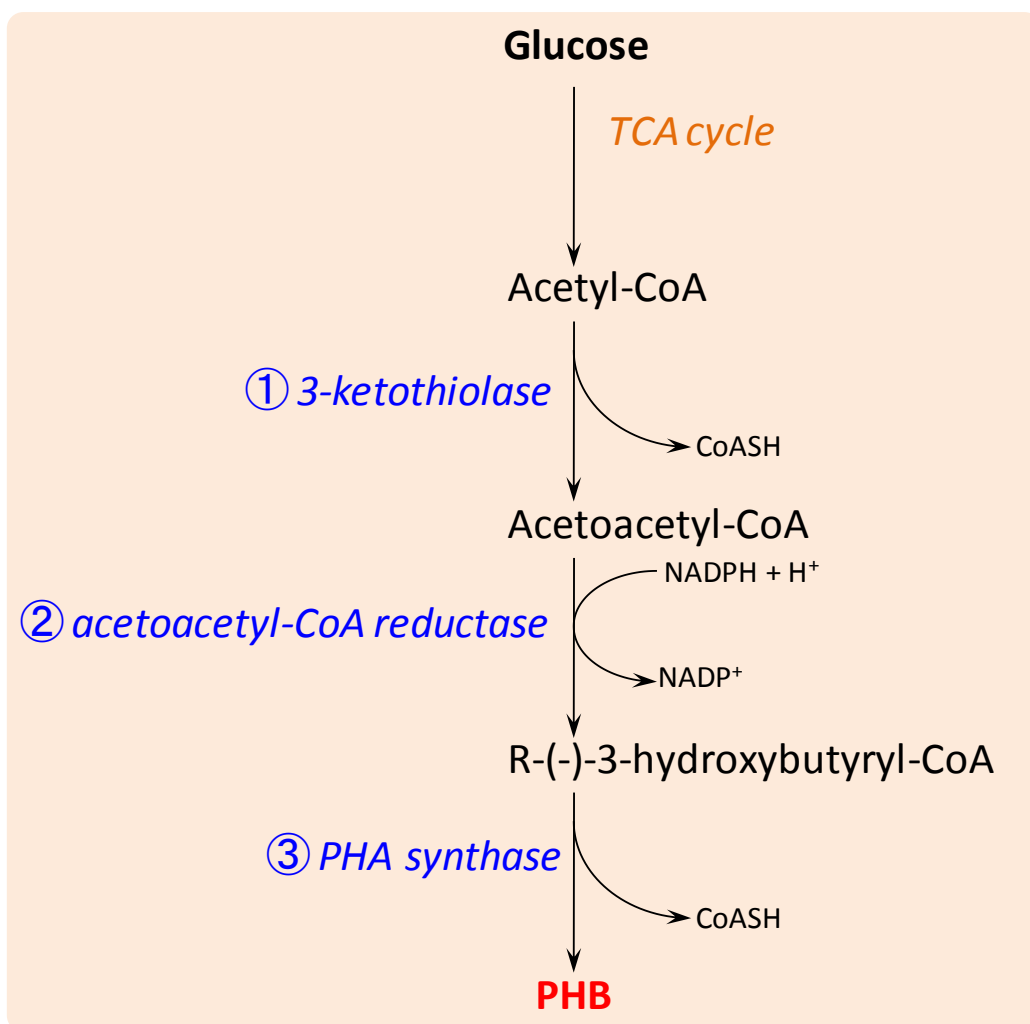


Figure 1.2 : PHB synthetic pathway in *A. eutrophus*.⁵

II. Biodegradable polymers produced from natural products and their derivatives

The biodegradability of commodity synthetic polymers can be increased by blending them with several types of natural products, such as starch and chitin. Ratto et al. prepared films from a poly(butylene succinate/adipate) (PBSA)/starch composite and investigated the processability and biodegradability of the resulting films, along with their mechanical and thermal properties.¹⁶ The biodegradable PBSA/starch film exhibited enough mechanical properties for plastic extrusion applications.

Although chitin is one of the most abundant natural products next to cellulose, its poor solubility and reactivity have limited its industrial use. To solve this problem, chitin has been chemically modified by grafting with synthetic polymers to improve its miscibility with various commodity polymers.³ Aoi et al. have synthesized chitin derivatives containing polyoxazoline side chains and prepared miscible blends containing synthetic polymers, such as polyvinyl chloride and polyvinyl alcohol.^{17,18} These blends are expected to be widely used as new polymeric materials not only for their biodegradability but also for the moulding and mechanical properties similar to that of commodity polymers.^{17,18}

In addition, PHB (Section I) has also been produced in the leaf of transgenic plants such as *Arabidopsis thaliana*.¹⁹ This plant-mediated synthesis was justified by its potential for a larger scale and a lower cost production than bacterial fermentation.⁵ As reported by Proirer et al.,^{5,20} out of the three enzymes required for PHB synthesis from acetyl-CoA, only the first enzyme 3-ketotiolase was endogenously present in plants. To achieve the PHB synthetic pathway in plants, the *A. eutrophus* genes encoding acetoacetyl-CoA reductase and PHA synthase were expressed in transgenic *A.*

thaliana.

III. Biodegradable polymers produced via chemical synthesis

This group mainly consists of aliphatic polyesters, such as polyglycolic acid (PGA), polylactic acid (PLA), polycaprolactone (PCL), and PBSA. These polymers are synthesized commonly through metal-catalyzed ring-opening polymerization (ROP) or polycondensation of their corresponding petroleum-derived monomers.^{2,3} Among these polymers, PLA, which can be prepared from natural products, such as cereal- or sugarcane-based saccharides, as well as petroleum precursors, has attracted tremendous attention as a biopolymer.^{21,22} Lactic acid that is obtained from glucose or sucrose via lactobacillus fermentation is polymerized by ROP after dimerization or direct polycondensation. PLA typically shows high rigidity, making it a suitable replacement for polystyrene and polyethylene terephthalate (PET) in several applications, such as packaging and textiles.^{21,23}

Similarly, synthesized by polycondensation of 1,4-butanediol and succinic acid, poly(butylene succinate) (PBS) has found use in a wide variety of applications, because the physical properties of PBS resemble those of commodity polymers, such as polyethylene (PE) and polypropylene (PP). Furthermore, comonomers, such as butylene adipate units, are often introduced into PBS polymer chains to improve its toughness and flexibility. The resulting copolyester, PBSA, also finds several uses, such as agricultural and construction materials.¹

As mentioned above, various types of biodegradable polymers are utilized in numerous fields ranging from agricultural to biomedical applications. With the growing awareness of waste management and environmental preservation,

biodegradable polymers are expected to reduce and eventually replace current commodity polymeric materials in practical use. The synthesis and/or modification of biodegradable polymers with improved physical and mechanical properties has also attracted significant interest. In the foreseeable future, the effective production of polymers exhibiting improved properties at reduced costs may become all the more crucial for realizing a sustainable society.

References

1. Y. Ichikawa and T. Mizukoshi, *Adv. Polym. Sci.*, **245**, 285-314 (2012).
2. G. E. Luckachan and C. K. S. Pillai, *J. Polym. Environ.*, **19**, 637-676 (2011).
3. M. Flieger, M. Kantorova, A. Prell, T. Rezanka, and J. Votruba, *Folia Microbiol.*, **48**, 27-44 (2003).
4. K. Sudesh, H. Abe, and Y. Doi, *Prog. Polym. Sci.*, **25**, 1503-1555 (2000).
5. Y. Proirier C. Nawrath, and C. Sommerville, *Nature Biotechnol.*, **13**, 142-150 (1995).
6. M. Nurbas and T. Kutsal, *Iranian Polym. J.*, **13**, 45-51 (2004).
7. A. J. Anderson and E. A. Dawes, *Microbiol. Rev.*, **40**, 450-472 (1990).
8. I. Y. Lee, G. J. Kim, D. K. Choi, B. K. Yeon, and Y. H. Park. *J. Ferment. Bioeng.*, **81**, 255-258 (1996).
9. S. O. Kulkarni, P. P. Kanekar, S. S. Nilegaonkar, S. S. Sarnaik, and J. P. Jog, *Bioresource Technol.*, **101**, 9765-9771 (2010).
10. Y. Wei, W. Chen, C. Huang, H. Wu, Y. Sun, C. Lo, and O. Janarthanan, *Int. J. Mo. Sci.*, **12**, 252-265 (2011).
11. R. A. J. Verlinden, D. J. Hill, M. A. Kenward, C. D. Williams, and I. Radecka, *J. Appl. Microbiol.*, **102**, 1437-1449 (2007).
12. M. Hamcerencu, J. Desbrieres, A. Khoukh, M. Popa, and G. Riess, *Carbohydrate Polym.*, **71**, 92-100 (2008).
13. D. F. Coutinho, S. V. Sant, H. Shin, J. T. Oliveira, M. E. Gomes, N. M. Neves, A. Khademhosseini, and R. L. Reis, *Biomaterials*, **31**, 7494-7502 (2010).
14. H. Marubayashi, K. Yukinaka, Y. Enomoto-Rogers, A. Takemura, and T. Iwata, *Carbohydr. Polym.*, **103**, 427-433 (2014).

15. G. Xiao, Y. Zhu, L. Wang, Q. You, P. Hao, and Y. You, *Procedia Environ. Sci.*, **8**, 756-763 (2011).
16. J. A. Ratto, P. J. Stenhouse, M. Auerbach, J. Mitchell, and R. Farrell, *Polymer*, **40**, 6777-6788 (1999).
17. K. Aoi, A. Takasu, and M. Okada, *Macromol. Rapid Commun.*, **16**, 53-58 (1995).
18. K. Aoi, A. Takasu, and M. Okada, *Macromol. Rapid Commun.*, **16**, 757-761 (1995).
19. L. Kourtz, K. Dillon, S. Daughtry, O. P. Peoples, and K. D. Snell, *Transgenic Res.*, **16**, 759-769 (2007).
20. Y. Proirer, *Adv. Biochem. Eng. Biotechnol.*, **71**, 209-240 (2001).
21. K. O. Siegenthaler, A. Kunkel, G. Skupin, and M. Yamamoto, *Adv. Polym. Sci.*, **245**, 91-136 (2012).
22. D. Briassoulis and C. Dejean, *J. Polym. Environ.*, **18**, 384-400 (2010).
23. P. Lecomte and C. Jerome, *Adv. Polym. Sci.*, **245**, 173-218 (2012).

1.2 Importance of the compositional analysis of biodegradable copolyesters

Physical properties of biodegradable polymers, such as melting point, glass transition temperature, crystallinity, and transparency, depend on their molecular structural features.¹ In the case of copolymers, they also rest on the chemical composition.²⁻⁴ Many reports have detailed the relationship between the copolymer composition and physical properties for various biodegradable PBS-based copolyesters, such as poly(butylene succinate-*co*-butylene adipate) [P(BS-*co*-BA)],⁵⁻⁹ poly(butylene succinate-*co*-ethylene succinate) [P(BS-*co*-ES)],¹⁰ and poly(butylenesuccinate-*co*-butylenesebacate) [P(BSu-*co*-BSe)].¹¹ Copolyesters involving poly(3-hydroxybutyrate) (P3HB) moieties, such as poly(3-hydroxybutyrate-*co*-3-hydroxyvalerate) [P(3HB-*co*-3HV)],¹²⁻¹⁴ poly(3-hydroxybutyrate-*co*-4-hydroxyvalerate) [P(3HB-*co*-4HB)],¹⁵⁻¹⁷ and poly(3-hydroxybutyrate-*co*-2-hydroxypropionate) [P(3HB-*co*-2HP)],¹⁸ have also been extensively studied. Ahn et al.⁷ have related the copolymer composition of P(BS-*co*-BA) with several physical properties and found that the melting point (T_m) and glass-transition temperature (T_g) decreased gradually when the BA content in the polymer chains increased. In addition, their crystallinity (X_c), which is determined by differential scanning calorimetry (DSC), decreased to 25% when the BA composition reached to approximately 50 mol%. Tabata et al.¹⁸ studied the effects of the structural features and chemical composition on the thermal properties of P(3HB-*co*-2HP). The T_g values of the copolyesters were mainly governed by the copolymer composition and increased linearly with the composition of 2HP units. Also, X_c values were affected by the composition and sequential length of the crystallizable monomeric unit.

Moreover, the copolymer composition of biodegradable copolyesters strongly

affects their biodegradability.⁵⁻¹⁸ Ishioka et al.⁸ have reported that the rate of biodegradation of PBS increased significantly upon introduction of BA comonomer into the polymer chains because of the reduced crystallinity. This approach has produced the biodegradable copolyesters Bionolle #3001 and #3020, which exhibit enhanced biodegradability compared to the PBS homopolymer.⁸ Many researchers have studied the correlation between copolymer composition and biodegradability for PBS-based copolyesters.⁵⁻⁹ Nikolic et al.⁹ have evaluated the effect of P(BS-*co*-BA) film composition on their enzymatic degradation. The enzymatic degradation was performed using *Candida cylindracea* lipase in a buffer solution at 30°C for 90 h. The biodegradability of the copolyesters was determined by monitoring the weight loss of the P(BS-*co*-BA) films over time. Copolyesters with lower BS content (up to 50 mol%) degraded significantly because of their reduced crystallinity, while those presenting a higher BS content (75 mol%) showed little enzymatic weight loss under the employed experimental conditions.

Tserki et al.⁵ also evaluated the biodegradability of P(BS-*co*-BA) for various BA compositions (20–80 mol%). Copolyester films were subjected to either a soil burial test for approximately 5 months or an enzymatic hydrolysis test for 15 days at 30-37°C in the presence of *Candida cylindracea* lipase, *Rhizopus delemar* lipase, and *Pseudomonas fluorescens* cholesterol esterase. Regardless of the degradation method and the type of enzyme, PBSA films displaying a quasi-equimolar composition (BS/BA = 50/50 and 40/60) showed higher biodegradation rates because of their reduced degree of crystallinity.

As for polyhydroxyalkanoate-based copolyesters, Kasuya et al.¹² discovered that the introduction of comonomers, such as 3HV units, enhanced the biodegradability

of P3HB. Biosynthetic P(3HB-*co*-14% 3-HV) films degraded rapidly in all natural waters, such as river, lake, and sea water, with a quantitative weight loss in 28 days at 25°C, indicating that they were completely hydrolyzed into watersoluble products by microorganisms.

As described above, the compositional data of biodegradable copolyesters often provides useful clues for biodegradability prediction. Furthermore, it gives a good measure of the degree of biodegradation as long as the composition changes gradually during the biodegradation. These benefits have led to a growing demand for accurate and precise determination of biodegradable copolyester composition. Various analytical approaches, such as spectroscopic methods and conventional chromatographic techniques, have been used to achieve this goal. Nuclear magnetic resonance (NMR) spectroscopy and post-transmethylation gas chromatography (GC) are the most utilized characterization techniques. Their applications and limitations are briefly discussed below.

I. Nuclear magnetic resonance (NMR) spectroscopy

¹H-NMR spectroscopy is extensively used by chemists and biochemists to investigate the chemical structure of numerous polymeric materials. Furthermore, it has proven a method of choice to analyze the chemical composition of biodegradable copolyesters.^{5-7,9-11,15,17,18} Nikolic et al.⁹ characterized the structure and average molecular weight of P(BS-*co*-BA) by ¹H-NMR (200 MHz). The copolyester composition was also determined from the relative intensities of the proton peaks arising from the succinate and adipate repeating units.

Moreover, Montaudo et al.¹¹ synthesized and characterized a series of aliphatic

copolyesters with number-average molecular weights ranging from 33,000 up to 85,000. The copolyesters consisted of 1,4-butanediol units paired with succinic, adipic and sebacic acid units. Their compositions were calculated by integrating the $^1\text{H-NMR}$ signals attributed to butylene succinate (2.628 ppm), butylene sebacate (2.294 ppm), and butylene adipate (2.332 ppm). The obtained composition values were in good agreement with the feed ratio used in the synthesis.

Although NMR provides accurate and precise compositional data for biodegradable copolyesters, NMR is unsuitable for routine analyses, because it requires a relatively large sample size (a few tens of milligrams). Moreover, the NMR characterization of highly crystalline polymers, such as P(3HB), PBS and chitin/chitosan, is cumbersome because of their low solubilities in solvents.

II. Post-transmethylation Gas Chromatography (GC)

The chemical composition of copolymers has been also analyzed by gas chromatography after preliminary sample pretreatments, such as transmethylation and solvent extraction. So far, this technique has been widely applied to determine the composition of various biodegradable copolyesters, such as PHB¹⁶ and P(HB-*co*-HV).¹⁵⁻¹⁷

Furthermore, it has proven to be a powerful tool to analyze the amount and chemical composition of biodegradable polyesters accumulated in bacteria.^{15-17,19-22} The sample pretreatment procedure developed by Brauneegg et al.²³ in the 1970s remains useful for polyester characterization in bacteria. In this method, centrifuged bacterial cells were suspended in a mixture of acidic methanol (ca. 10% H_2SO_4) and chloroform. Next the mixture was heated to about 100°C for a few hours to depolymerize the

polyesters present in the cells into its constituent monomers by transmethylation. After cooling to room temperature, transmethylated monomers were isolated by liquid–liquid extraction using water as a medium and subsequently analyzed by GC.

This GC technique, however, required a fairly large amount of sample (at least 20 mg) and relatively long sample pretreatment time (approximately half a day) prior to a final GC measurement.

Existing analytical techniques used for the compositional analysis of biodegradable copolyesters present advantages and drawbacks regarding convenience and sensitivity. Therefore, a practical and highly sensitive method is needed to meet this challenge.

References

1. G. E. Luckachan and C. K. S. Pillai, *J. Polym. Environ.*, **19**, 637-676 (2001).
2. D. Briassoulis, *J. Polym. Environ.*, **12**, 65-81 (2004).
3. A. A. Shah, F. Hasan, A. Hameed, and S. Ahmed, *Biotech. Adv.*, **26**, 246-265 (2008).
4. R. A. J. Verlinden, D. J. Hill, M. A. Kenward, C. D. Williams, and I. Radecka, *J. Appl. Microbiol.*, **102**, 1437-1449 (2007).
5. V. Tserki, P. Matzinos, E. Pavlidou, D. Vachliotis, and C. Panayiotou, *Poly. Deg. Stab.*, **91**, 367-376 (2006).
6. V. Tserki, P. Matzinos, E. Pavlidou, and C. Panayiotou, *Poly. Deg. Stab.*, **91**, 377-384 (2006).
7. B. D. Ahn, S. H. Kim, Y. H. Kim, and J. S. Yang, *J. Appl. Polym. Sci.*, **82**, 2808-2826 (2001).
8. R. Ishioka, E. Kitakuni, and Y. Ichikawa, in "Biopolymers Online", A. Steinbuechel ed., Wiley-VCH Verlag GmbH & Co. KGaA, p.275-297, 2005 (10. Aliphatic Polyesters : Bionolle).
9. M. S. Nikolic and J. Djonlagic, *Polym. Deg. Stab.*, **74**, 263-270 (2001).
10. M. Mochizuki, K. Mukai, K. Yamada, N. Ichise, S. Murase, and Y. Iwaya, *Macromolecules*, **30**, 7403-7407 (1997).
11. G. Montaudo and P. Rizzarelli, *Polym. Deg. Stab.*, **70**, 305-314 (2000).
12. K. Kasuya, K. Takagi, S. Ishiwari, Y. Yoshida, and Y. Doi, *Polym. Deg. Stab.*, **59**, 327-332 (1998).
13. M. J. Fabra, G. Sanchez, A. Lopez-Rubio, and J. M. Lagaron, *Food Sci. Technol.*, **59**, 760-767 (2014).

14. T. Ishigaki, W. Sugano, A. Nakanishi, M. Tateda, M. Ike, and M. Fujita, *Chemosphere*, **54**, 225-233 (2004).
15. U. Rao, R. Sirdar, and P. K. Segal, *Biochem. Eng. J.*, **49**, 13-20 (2010).
16. E. Y. Lee and C. Y. Choi, *Biotechnol. Tech.*, **11**, 167-171 (1997).
17. H. Chai, R. Ahmad, A. R. M. Yahaya, M. I. A. Majid, and A. A. Amirul, *Afr. J. Biotechnol.*, **8**, 4089-4196 (2009).
18. Y. Tabata and H. Abe, *Polym. Deg. Stab.*, **98**, 1796-1803 (2013).
19. A. Degelau, T. Scheper, J. Bailey, and C. Guske, *Appl. Microbiol. Biotechnol.*, **42**, 653-657 (1995).
20. A. Betancourt, A. Yezza, A. Halasz, H. V. Tra, and J. Hawari, *J. Chromatogr. A*, **1154**, 473-476 (2007)
21. K. Sangkharak and P. Prasertsan, *Electron. J. Biotechnol.*, **11**, 1-12 (2008).
22. G. Braunegg, B. Sonnleitner, and R. M. Lafferty, *European J. Appl. Microbiol. Biotechnol.*, **6**, 29-37 (1978).

1.3 Compositional Analysis of Copolymers by Reactive Pyrolysis-Gas Chromatography (Reactive Py-GC)

1.3.1 Pyrolysis-Gas Chromatography (Py-GC)

Among analytical techniques, pyrolysis-gas chromatography (Py-GC) has been increasingly utilized as a practical tool for the structural characterization of synthetic polymers and natural organic compounds in a variety of fields including polymer chemistry, biochemistry, and environmental sciences.¹⁻¹¹ This technique enables rapid and highly-sensitive characterization without using any tedious and time-consuming sample pretreatment, even for insoluble samples. In Py-GC measurements, a given polymer or organic compound sample weighing about 10–100 µg is instantaneously pyrolyzed at high temperature around 500 or 600°C under a flow of helium or nitrogen carrier gas. The resulting degradation products are transferred directly into the separation column of a GC system where they are separated to yield a chromatogram called a “pyrogram.” The detailed structural characterization and/or precise compositional analysis of the original sample can often be carried out on the basis of the obtained pyrogram.

However, conventional Py-GC does not necessarily provide any useful information for condensation polymers due to their lower decomposition efficiencies, which result in the formation of large amounts of solid residues and chars after pyrolysis. Furthermore, even if these polymer samples are pyrolyzed to some extent, the major thermal decomposition products are a series of polar compounds containing carboxylic and/or hydroxyl groups, which are not amenable to GC separation. As a consequence, the precise compositional analyses of condensation polymers such as polyesters based

on pyrograms are usually difficult as only broad peaks of the polar components with weak intensities are observed.⁸

1.3.2 Reactive Pyrolysis-Gas Chromatography (Reactive Py-GC)

In 1989, Challinor reported that the Py-GC method in the presence of organic alkali such as tetramethylammonium hydroxide (TMAH) is effective for the analysis of synthetic polymers and natural organic compounds containing ester bonds and/or polar groups.¹² During pyrolysis in the presence of TMAH, only ester bonds or ether bonds in the sample components are hydrolyzed and subsequently methylated to yield their corresponding methyl derivatives, while carbon-carbon bonds are maintained. Based on the extremely simplified pyrograms consisting mainly of the methyl derivatives of the sample constituents, the qualitative and quantitative analysis of the sample can be performed without any cumbersome sample pretreatment. This report by Challinor greatly progressed the field of analytical pyrolysis, and this technique has since been applied to the successful characterization of condensation polymers^{6,12-16} and natural polar organic compounds such as lipids,¹⁷⁻²¹ natural resins,^{22,23} natural waxes,^{24,25} humic substances,^{26,27} and lignin.^{28,29}

TMAH, which is the most widely used organic alkali in reactive Py-GC, has several advantages:³⁰

- (1) TMAH can react with samples not only as hydrolysis reagent but also as a methylating reagent with high reaction efficiency;
- (2) TMAH itself is decomposed into tetramethylamine and methanol at temperatures above 130°C, which does not damage the separation column.

Figure 1.3 shows a possible mechanism of the reactive pyrolysis of an ester compound

in the presence of TMAH suggested by de Leeuw et al.³¹ As shown in this figure, the proposed reaction mechanism consists of three steps: first, an ester bond is hydrolyzed by the action of TMAH as a base, producing carboxylate anion and alcohol; second, these hydrolysis products (carboxylate anion and alcohol) react with tetramethylammonium ion and TMAH, respectively, to form their tetramethylammonium salts; and finally, these salts are thermally decomposed into their corresponding methyl ester and methyl ether with the release of trimethylamine.³¹ Various terms have been employed to describe the reactive pyrolysis of ester compounds in the presence of TMAH via the above-described mechanism, including thermochemolysis, on-line methylation, and thermally-assisted hydrolysis and methylation (THM).³²

To date, reactive Py-GC in the presence of TMAH has been adapted to the compositional analysis of various condensation polymers including multi-component liquid crystalline aromatic polyesters (LCs)^{33,34}, cationic polyacrylamide resins,³⁵ copolymer type polycarbonates (PCs),³⁶ poly(aryl ether sulfone),³⁷ and poly(3-hydroxybutyrate-*co*-3-hydroxyvalerate) [P(3HB-*co*-3HV)].^{27,38} Among these papers, Sato et al.³⁸ applied the reactive Py-GC method to the compositional analysis of a biodegradable copolyester, P(3HB-*co*-3HV), with a wide range of 3HV contents (ca. 4–23 mol%). The report by Sato et al. revealed that P(3HB-*co*-3HV) subjected to pyrolysis in the presence of TMAH at around 350°C underwent not only the typical reactive pyrolysis, but also the *cis*-elimination of the ester linkages followed by the hydrolysis and methylation of the adjacent ester bond. Based on the peak intensities of the product formed from these reactions, the copolymer composition was precisely analyzed without the use of any cumbersome pretreatment procedure. Furthermore,

the obtained copolymer compositions were consistent with those determined by $^1\text{H-NMR}$.

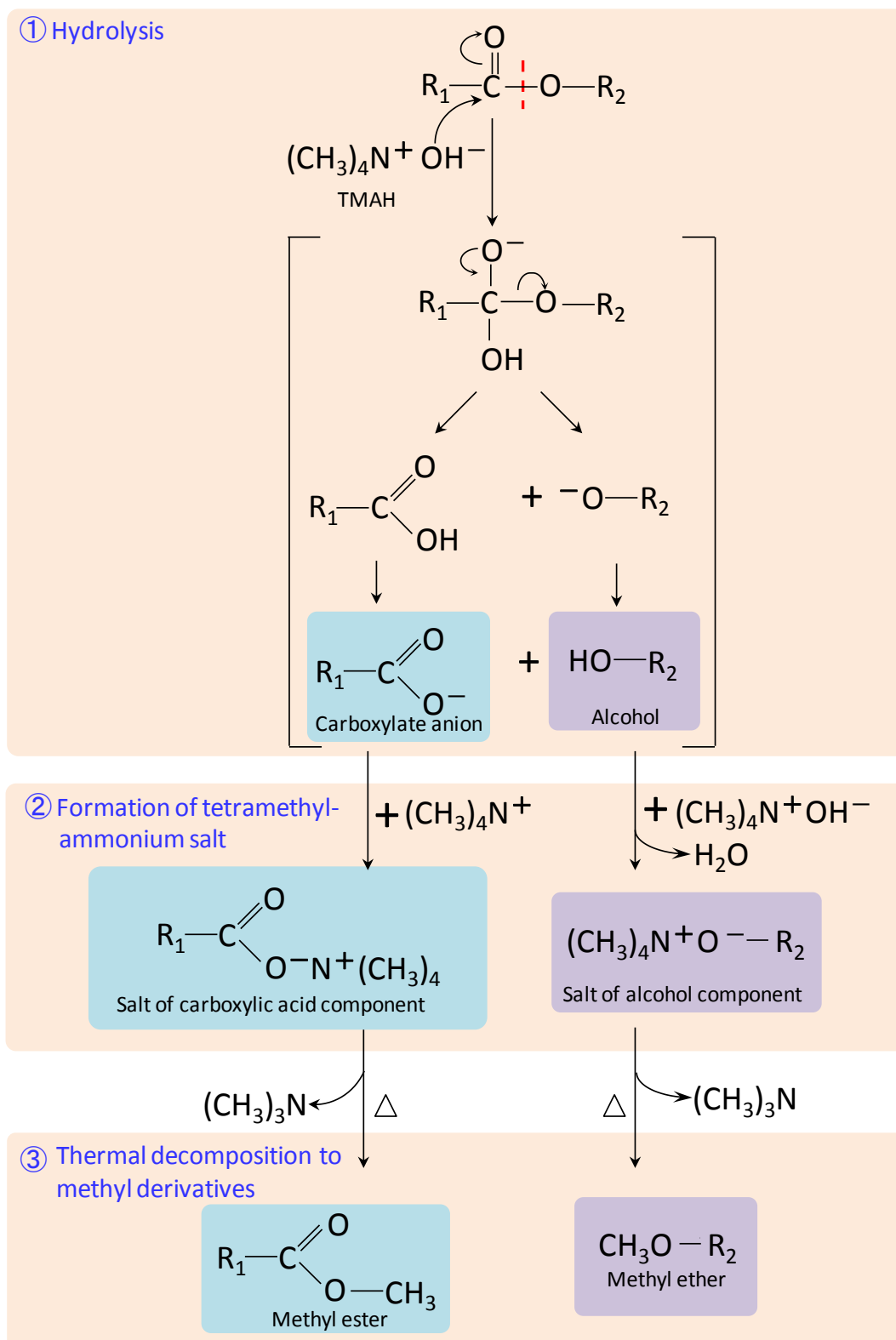


Figure 1.3: Proposed mechanism for the reactive pyrolysis of an ester compound in the presence of TMAH.³¹

References

1. S. Tsuge and H. Ohtani, in “Applied Pyrolysis Handbook”, T. P. Wampler ed., Marcel Dekker, New York, p. 77-124, 1995 (4. Microstructure of Polyolefins and 5. Degradation Mechanism of Condensation Polymers) .
2. S. Tsuge, J. Anal. Appl. Pyrolysis, **32**, 1-6 (1995).
3. H. Ohtani, Bunseki Kagaku, **45**, 135-156 (1996).
4. S. Tsuge and H. Ohtani, Polym. Degrad. Stab., **58**, 109-130 (1997).
5. S. Tsuge and H. Ohtani, in “Mass Spectrometry of Polymers”, G. Montaudo, and R. P. Lattimer ed., CRC Press, p.113-147, 2001 (3. Pyrolysis Gas Chromatography/Mass Spectrometry (Py-GC/MS)) .
6. S. Tsuge, H. Ohtani, and C. Watanabe, “Pyrolysis-GC/MS Data Book of Synthetic Polymers – Pyrograms, Thermograms and MS of Pyrolyzates”, Elsevier Publication, United Kingdom, 2011.
7. E. Kaal and H. G. Janssen, J. Chromatogr. A, **1184**, 43-60 (2008).
8. K. L. Sobeih, M. Baron, and J. G. Rodriguez, J. Chromatogr. A, **1186**, 51-66 (2008).
9. J. K. Haken, J. Chromatogr. A, **825**, 171-187 (1998).
10. T. A. Brettel, in “Modern Practice of Gas Chromatography”, R. L. Grob, and E. F. Barry ed., John Wiley & Sons. Inc., p. 882-968, 2004 (16. Forensic Science Application of Gas Chromatography).
11. R. R. Otero, M. Galesio, J. L. Capelo, and J. S. Gandara, Chromatographia, **70**, 339-348 (2009).
12. J. M. Challinor, J. Anal. Appl. Pyrolysis, **16**, 323-333 (1989).
13. J. M. Challinor, J. Anal. Appl. Pyrolysis, **20**, 15-24 (1991).
14. Y. Ishida, H. Ohtani, and S. Tsuge, Bunseki Kagaku, **47**, 673-688 (1998).

15. J. M. Challinor, *J. Anal. Appl. Pyrolysis*, **61**, 3-34 (2001).
16. F. Shadkami and R. Helleur, *J. Anal. Appl. Pyrolysis*, **89**, 2-16 (2010).
17. J. P. Dworzanski, L. Berwald, and H. L. C. Meuzelaar, *Appl. Environ. Microbiol.*, **56**, 1717-1724 (1990).
18. J. P. Dworzanski, L. Berwald, W. H. McClennen, and H. L. C. Meuzelaar, *J. Anal. Appl. Pyrolysis*, **21**, 221-232 (1991)
19. Y. Ishida, K. Kitagawa, A. Nakayama, and H. Ohtani, *J. Anal. Appl. Pyrolysis*, **77**, 116-120 (2006).
20. Y. Ishida, T. Honda, S. Mabuchi, and O. Sueno, *J. Agri. Food. Chem.*, **60**, 4222-4226 (2012).
21. Y. Ishida, S. Wakamatsu, H. Yokoi, H. Ohtani, and S. Tsuge, *J. Anal. Appl. Pyrolysis*, **49**, 267-276 (1999).
22. J. M. Challinor, *J. Anal. Appl. Pyrolysis*, **25**, 349-360 (1993).
23. L. Wang, Y. Ishida, H. Ohtani, S. Tsuge, and T. Nakayama, *Anal. Chem.*, **71**, 1316-1322 (1999).
24. A. Asperger, W. Engewald, and G. Fabian, *J. Anal. Appl. Pyrolysis*, **52**, 51-63 (1999).
25. L. Wang, S. Ando, Y. Ishida, H. Ohtani, S. Tsuge, and T. Nakayama, *J. Anal. Appl. Pyrolysis*, **58-59**, 525-537 (2001).
26. J. C. de Rio, F. J. Gonzales-Vila, F. Martin, and T. Verdejo, *Org. Geochem.*, **22**, 885-891 (1994).
27. F. Martin, J. C. de Rio, F. J. Gonzales-Vila, and T. Verdejo, *J. Anal. Appl. Pyrolysis*, **31**, 75-83 (1995).
28. K. Kuroda and A. Nakagawa-izumi, *Org. Geochem.*, **36**, 53-61, (2005).

29. K. Kuroda, A. Nakagawa-izumi, T. Ashitani, and K. Fujita, *J. Anal. Appl. Pyrolysis*, **86**, 185-191 (2009).
30. J. Imamura, C. Aoba, and K. Kojima, *J. Syn. Org. Chem.*, **45**, 909-913 (1987).
31. J. W. de Leeuw and M. Baas, *J. Anal. Appl. Pyrolysis*, **26**, 175-184 (1993).
32. J. M. Challinor, *J. Anal. Appl. Pyrolysis*, **29**, 223-224 (1994).
33. H. Ohtani, N. Sugimoto, M. Hirano, T. Yokota, and K. Katoh, *J. Anal. Appl. Pyrolysis*, **79**, 323-326 (2007) .
34. H. Ohtani, R. Fujii, and S. Tsuge, *J. High Res. Chromatog.*, **14**, 388-391 (1991).
35. Y. Ishida, S. Tsuge, H. Ohtani, F. Inokuchi, Y. Fujii, and S. Suetomo, *Anal. Sci.*, **12**, 835-838 (1996).
36. Y. Ishida, S. Kawaguchi, Y. Ito, S. Tsuge, and H. Ohtani, *J. Anal. Appl. Pyrolysis*, **40-41**, 321-329 (1997).
37. H. Ohtani, Y. Ishida, M. Ushiba, and S. Tsuge, *J. Anal. Appl. Pyrolysis*, **61**, 35-44 (2001).
38. H. Sato, M. Hoshino, H. Aoi, T. Seino, Y. Ishida, K. Aoi, and H. Ohtani, *J. Anal. Appl. Pyrolysis*, **74**, 193-199 (2005).

1.4 Objectives of the Present Research

As described in the previous section, reactive Py-GC in the presence of TMAH has proven to be a rapid and highly sensitive method to determine the copolymer compositions of condensation polymers without any cumbersome pretreatment. However, for biodegradable copolyesters, there have been few reports on their precise compositional analysis by reactive Py-GC. This is due to the lack of fundamental studies on the optimization of operating conditions such as temperature and amount of reagent required to obtain the highly-efficient reactive pyrolysis of biodegradable copolyesters.

This dissertation describes studies focused on the **highly sensitive compositional analysis of biodegradable copolyesters by reactive Py-GC**. First, a method for the precise and sensitive compositional analysis of biodegradable copolyesters was developed by optimizing the operating conditions of reactive Py-GC. The resulting copolymer compositional data were validated by comparing them with the data obtained by conventional methods such as NMR and GC after transmethylation. Furthermore, the compositional data were interpreted in terms of the evaluation of (1) the degree of biodegradability for poly(butylene succinate-*co*-butylene adipate) [P(BS-*co*-BA)] and (2) the direct characterization of poly(3-hydroxybutyrate-*co*-3-hydroxyvalerate) [P(3HB-*co*-3HV)] accumulated in whole bacterial cells.

In Chapter 1, the current methods used for the compositional analysis of biodegradable copolyesters are briefly described. The specific features of reactive Py-GC are then discussed.

In Chapter 2, the compositional analysis and evaluation of the biodegradability of P(BS-*co*-BA) are described in detail. The compositional analysis of P(BS-*co*-BA)

was carried out precisely using reactive Py-GC under the optimized operating conditions. The biodegradability of P(BS-*co*-BA) was then evaluated based on its copolymer composition determined by reactive Py-GC using trace amounts (20 µg) of film samples. The obtained data were correlated with the biodegradability of the P(BS-*co*-BA) film samples during a soil burial biodegradation test. As a result, the copolymer compositions of butylene adipate (BA) units gradually decreased with soil burial. Furthermore, the local differences in the biodegradability of a given P(BS-*co*-BA) film sample after soil burial were successfully evaluated based on the copolymer compositions.

In Chapter 3, the cause of the decrease in BA content of the P(BS-*co*-BA) films with soil burial degradation time observed in Chapter 2 is clarified in detail. P(BS-*co*-BA) film samples with lower degrees of crystallinity were prepared by heating and quickly cooling the original commercially available films and then subjected to a soil burial degradation test under conditions similar to those utilized in the previous chapter. The reactive Py-GC measurements of the degraded film samples revealed that the changes in copolymer compositions of the heated P(BS-*co*-BA) films during soil burial were relatively small compared to the original films. This suggests that biodegradation rates for the heated films with both BA- and BS-rich moieties were comparable due to lowered crystallinity. Based on these results, the reason for the change in copolymer composition observed in the original P(BS-*co*-BA) films was clarified.

In Chapter 4, reactive Py-GC in the presence of TMAH was applied to the direct compositional analysis of P(3HB-*co*-3HV) accumulated in whole bacterial cells. Trace amounts (30 µg) of dried *Cupriavidus necator* cells were directly subjected to

reactive Py-GC in the presence of TMAH at 400°C. The obtained chromatograms clearly showed a series of characteristic peaks attributed to the reactive pyrolysis products from the 3HB and 3HV units in the polymer chains without any appreciable interference from the bacterial matrix components. Based on the peak intensities, the copolymer compositions were determined rapidly without the use of any cumbersome sample pretreatment. Moreover, the obtained compositions were in good agreement with those obtained by the conventional technique.

In Chapter 5, the reactive Py-GC technique utilized for the compositional analysis of biodegradable copolyesters is summarized.

Chapter 2

Evaluation of Biodegradability of Poly(butylene succinate-*co*-butylene adipate) on the Basis of Copolymer Composition Determined by Reactive Pyrolysis-Gas Chromatography

2.1 Introduction

Poly(butylene succinate) (PBS) is a biodegradable semicrystalline polyester which is widely used as a packaging material owing to physical properties similar to those of commodity polymers such as polyethylene and polypropylene.^{1,2} Furthermore, in order to improve its toughness and flexibility, various comonomers such as butylene adipate (BA) units are often introduced into the polymer chains of PBS.^{1,3,4} Figure 2.1 shows the possible chemical structure of poly(butylene succinate-*co*-butylene adipate) [P(BS-*co*-BA)]. It is well known that the copolymer composition of P(BS-*co*-BA) controls its various properties, including biodegradability. In addition, the data for the composition might provide useful clues to elucidate the degradation mechanism of P(BS-*co*-BA).

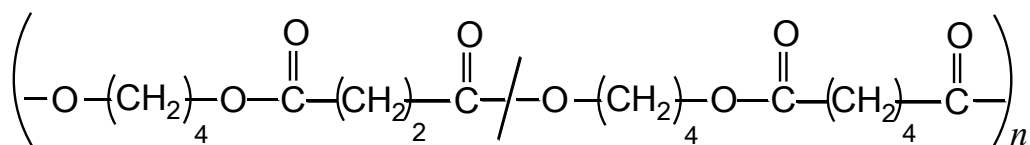


Figure 2.1 : Chemical structure of P(BS-*co*-BA).

As mentioned in Chapter 1.2, the compositional analysis of P(BS-*co*-BA) has been analyzed by nuclear magnetic resonance (NMR),^{5,6} Fourier transform-infrared absorption spectroscopy (FT-IR),⁷ and gas chromatographic (GC) measurement of the methanolysis products.⁸ However, these techniques are not always applied for routine analysis because of the relatively large amount of sample and fairly long measuring

time, including that required for sample preparation. Pyrolysis-gas chromatography (Py-GC) was also applied to the structural analysis of P(BS-*co*-BA).⁹ The resulting pyrogram mainly showed a series of peaks mainly attributed to ester compounds composed of the monomeric units of the polymer chains. The changes in the chemical structure of P(BS-*co*-BA) during soil burial degradation were analyzed in detail based on variations in the yields of these pyrolysis products observed on the pyrograms. However, data for the copolymer composition were not obtained, mainly because of the complexity of pyrograms

In this study, we tried a highly-sensitive and precise compositional analysis of P(BS-*co*-BA) by means of reactive Py-GC in the presence of TMAH. First, the data for copolymer composition of P(BS-*co*-BA) films, which was obtained by reactive Py-GC under the optimized conditions such as temperature, were compared with those by NMR for the sake of the validation. Then, reactive Py-GC was applied to the compositional analysis of the P(BS-*co*-BA) film samples after a soil burial biodegradation test to evaluate their biodegradability. Finally, the local variation of biodegradation in a given P(BS-*co*-BA) film subjected to soil burial was elucidated on the basis of changes in the copolymer compositions measured by reactive Py-GC.

2.2 Experimental

2.2.1 Materials

The industrially available biodegradable copolyester P(BS-*co*-BA) with the trade name Bionolle 3001 (Showa Highpolymer Co. Ltd., Japan) was used in this work. A small amount (approximately 0.5%) of hexamethylene diisocyanate units was also introduced into the P(BS-*co*-BA) in order to elongate the polymer chains. A methanol solution of tetramethylammonium hydroxide (TMAH) (2.2 M) purchased from Aldrich was used as an organic alkali reagent.

2.2.2 Soil Burial Biodegradation Test

Circular pieces (approximately 15 mg) of thin P(BS-*co*-BA) films (30 mm diameter, 35 μm thickness, Figure 2.2) were subjected to a soil burial biodegradation test for 1–4 weeks. The soil (pH 5.3) used in this study had been composted in the farm at Chubu University (Kasugai, Aichi Prefecture, Japan) and was contained in a small plastic container (schematically shown in Figure 2.3 and 2.4) in an incubator, in which the relative humidity was adjusted to approximately 90% and the temperature was kept constant at 30°C. After designated periods, each degraded P(BS-*co*-BA) film was washed with water, dried, and weighed. Here, the recovery (weight %) of each degraded film was calculated from its dry weight normalized by that of the original film before the burial test. Small discs (1 mm i.d.) weighing approximately 20 μg were cut from the degraded films using a Harris micropuncher (Frontier Laboratories) then subjected to reactive Py-GC measurements for evaluation of local biodegradation in the P(BS-*co*-BA) film samples. In addition, 2 ml of the chloroform solutions (10 mg/ml) of each residual film after the sampling of the local biodegradation test was used

in order to obtain the average chemical compositions of the P(BS-*co*-BA) film samples.



Figure 2.2 : Circular pieces of P(BS-*co*-BA) film sample before soil burial biodegradation test.



Figure 2.3 : Plastic containers used for soil burial biodegradation tests.

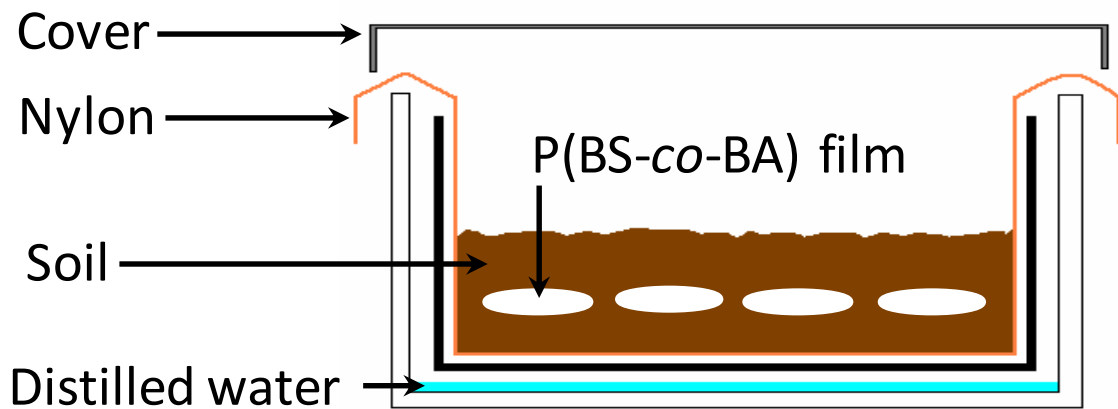


Figure 2.4 : Schematic diagram of plastic container used for soil burial biodegradation test.

2.2.3 Reactive Py-GC Measurement

Figure 2.5 shows a schematic diagram of the reactive Py-GC measurement system used in this study. A microfurnance pyrolyzer (Frontier Laboratories, PY-2010D), shown in Figure 2.6, was attached to a GC (Agilent, HP 4890) equipped with a flame ionization detector (FID). About 20 μg of the P(BS-*co*-BA) film sample was put into a small platinum cup (2 mm i.d. \times 4 mm height), and then 2 μl of the TMAH solution was added to the same sample cup as a methylating reagent. The sample cup was first mounted on the waiting position of the pyrolyzer near room temperature, and then dropped into the heated center of the pyrolyzer maintained at 350 $^{\circ}\text{C}$ under the flow of helium carrier gas (50 ml/min). A part of the flow (1 ml/min) reduced by a splitter was introduced into a metal capillary separation column (Frontier Laboratories, Ultra ALLOY-5 (MS/HT); 30 m long \times 0.25 mm i.d.) coated with immobilized 5% diphenyl-95% dimethylpolysiloxane (1.0 μm film thickness). The column temperature was programmed from 50 to 300 $^{\circ}\text{C}$ at a rate of 5 $^{\circ}\text{C}/\text{min}$. For peak identification, a GC-mass spectrometry (GC-MS) system (Shimadzu, QP-5050) with an electron ionization (EI) source was used.

2.2.4 $^1\text{H-NMR}$ measurement

$^1\text{H-NMR}$ spectra were obtained on a JEOL AL400 (400 MHz) spectrometer under the following conditions; spectral width of 8000 Hz, acquisition time of 4 s, relaxation time of 3 s and pulse width of 8.5 μs . About 5 mg of a sample dissolved in CDCl_3 (0.7 ml) was measured at room temperature. Chemical shifts were recorded in parts per million relative to the standard tetramethylsilane. The accumulation of 32 scans was used to obtain $^1\text{H-NMR}$ spectra having sufficient S/N values for the sample.

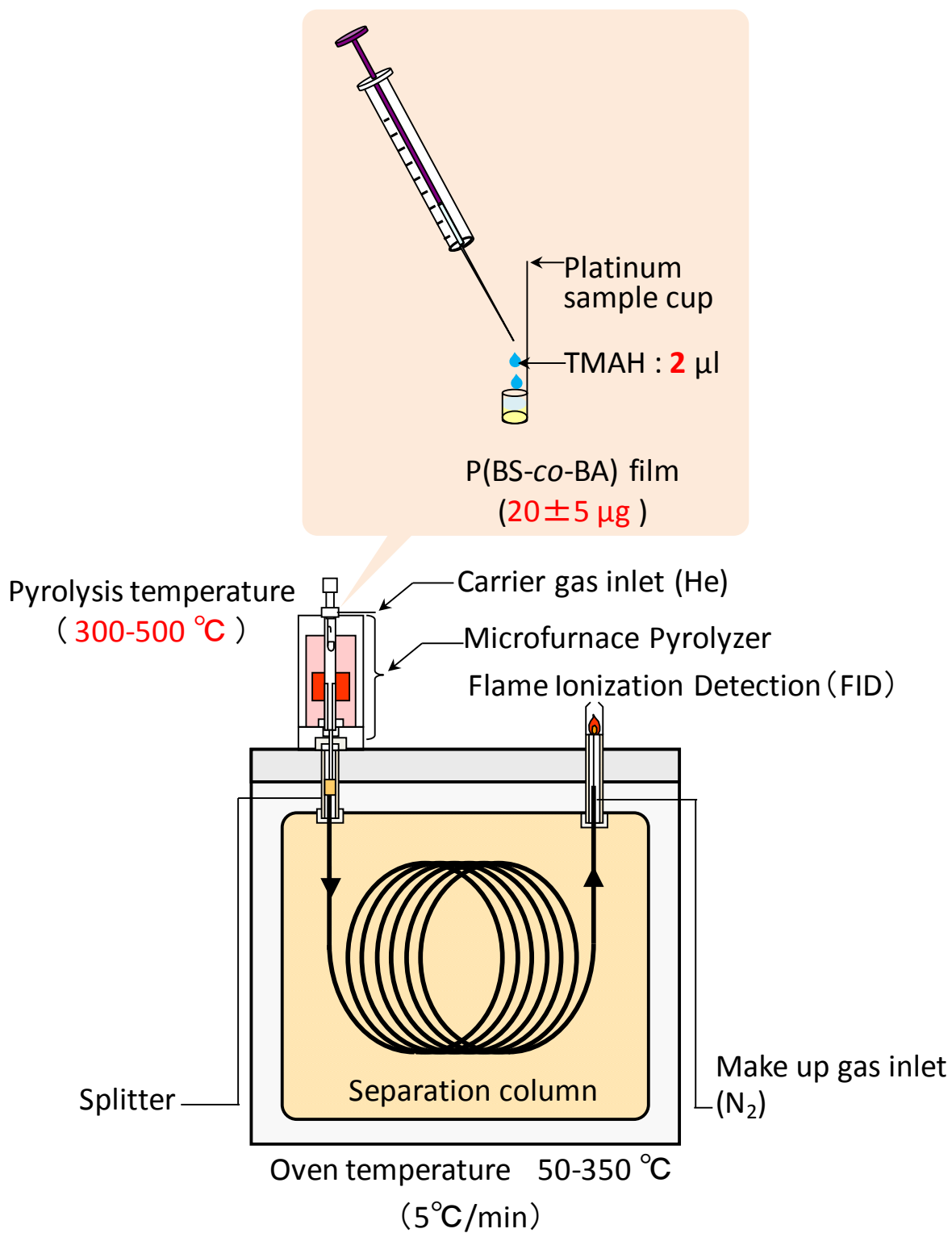


Figure 2.5 : Schematic diagram of reactive Py-GC measurement system.

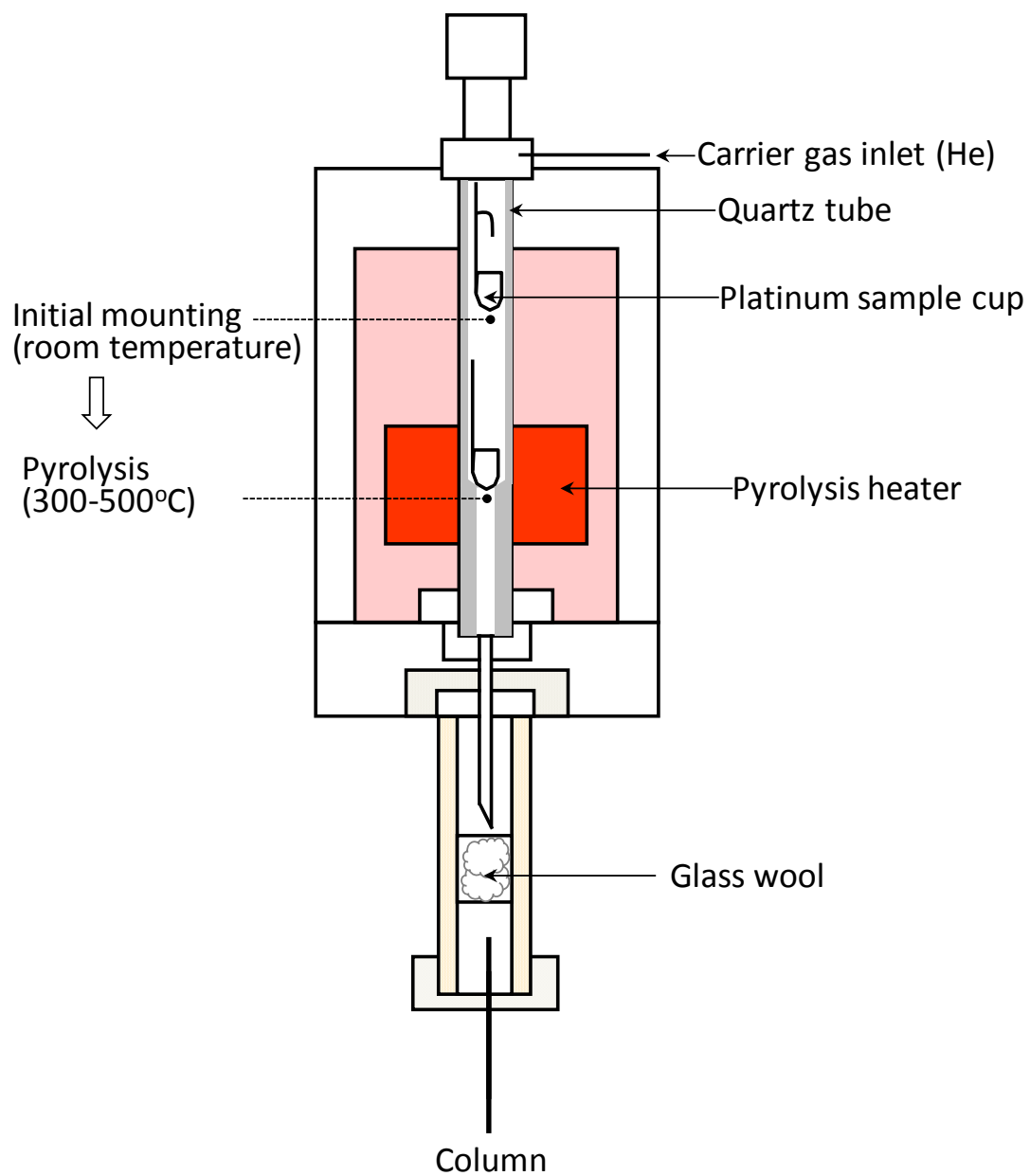


Figure 2.6 : Schematic diagram of a microfurnance pyrolyzer.

2.3 Results and Discussion

2.3.1 Compositional Analysis of the P(BS-*co*-BA) Samples

Figure 2.7 illustrates typical pyrograms of decomposition products from the original P(BS-*co*-BA) film sample obtained (a) by conventional pyrolysis without TMAH at 500°C and (b) through the reactive pyrolysis in the presence of TMAH at 350°C. As reported previously,⁹ the major products observed on the pyrograms in Figure 2.7 (a) were a series of ester compounds containing a succinate unit (S_x) and adipate unit (A_x), succinate dimers (SS), and hybrid dimers (SA). In addition, various low-molecular-weight products such as butene (B) and tetrahydrofuran (T_{HF}), originating from the 1,4-butandiol unit, and cyclopentanone (C_P), from the adipate unit, were also detected.⁹ However, precise compositional analysis was not possible based on their peak intensities because of (1) the complexity of the pyrograms consisting of many pyrolysis products, and (2) the possible formation of some other larger and/or polar products that cannot be detected in the pyrograms.

In contrast, on the pyrogram of Figure 2.7 (b), only four main peaks were clearly observed after the elution of TMAH-related products, including methanol and trimethylamine. Table 2.1 summarizes the assignments of these four peaks together with their molecular weights (MW) and effective carbon numbers (ECN) corresponding to the relative molar sensitivities for FID.¹⁰ The identified products were butanediol dimethyl ether (BD), butanediol monomethyl ether (BM), dimethyl succinate (SD), and dimethyl adipate (AD) formed through selective hydrolysis of ester linkages in the polymer chains followed by simultaneous methylation. In addition, some of the other small peaks appearing in this pyrograms might be derived from the hexamethylene diisocyanate units introduced into the P(BS-*co*-BA) chains.

Next, the effect of the reaction temperature on the reactive pyrolysis of the P(BS-*co*-BA) film samples was examined in detail. Figure 2.8 shows typical pyrograms of the P(BS-*co*-BA) film samples obtained by reactive Py-GC in the presence of TMAH at (a) 300°C, (b) 350°C, and (c) 500°C. On the pyrogram of (a), only small peaks were observed because of insufficient thermal energy to promote the reactive pyrolysis quantitatively. Moreover, the pyrogram of (c) showed some additional peaks generated by ordinary pyrolysis at an elevated temperature. On the contrary, on the pyrogram of (b), the four characteristics peaks derived from the backbones of P(BS-*co*-BA) were clearly observed with considerably high intensities. Furthermore, the observation that no other peak is detected in this pyrogram indicates that unwanted ordinary pyrolysis of P(BS-*co*-BA) does not occur during the reactive pyrolysis under this condition.

From the intensities of the SD and AD peaks obtained at 350°C, the copolymer compositions of BS and BA moieties in the P(BS-*co*-BA) samples, C_{BS} and C_{BA} (mol%), were calculated as follows:

$$C_{BS} \text{ (mol \%)} = [(P_{SD} / 3.5) / \{P_{SD} / 3.5\} + (P_{AD} / 5.5)\}] \times 100 \quad (1)$$

$$C_{BA} \text{ (mol \%)} = [(P_{AD} / 5.5) / \{P_{SD} / 3.5\} + (P_{AD} / 5.5)\}] \times 100 \quad (2)$$

where P_{SD} and P_{AD} are observed peak intensities of SD and AD, respectively. The values of 3.5 and 5.5 are the calculated ECNs of SD and AD shown in Table 2.1, respectively. According to Eqs. (1) and (2), the copolymer compositions of BA and

BS units for the original P(BS-*co*-BA) sample were estimated as 82.2 and 17.8 mol%. Moreover, the relative standard deviations for the observed copolymer compositions were less than 1% for five repeated runs of the reactive Py-GC measurements. Furthermore, the observed value for the copolymer composition of the P(BS-*co*-BA) film was compared with that obtained by ¹H-NMR. Figure 2.9 shows the ¹H-NMR spectrum of the P(BS-*co*-BA) film sample. On this spectrum, the peaks derived from methylene protons of adipate (3 and 5) and succinate (2) units were clearly appeared together with those of 1,4-butanediols units (1 and 4). The copolymer composition (BS/BA) calculated from the relative intensities of peaks 2 and 3 was 80/20, which was in fairly good agreement with that obtained by reactive Py-GC (82.2/17.8). These results indicate that the reactive Py-GC technique enables analyzing the copolymer compositions using very minute sample size, in the order of 20 μg of the P(BS-*co*-BA) sample, with sufficient accuracy and precision.

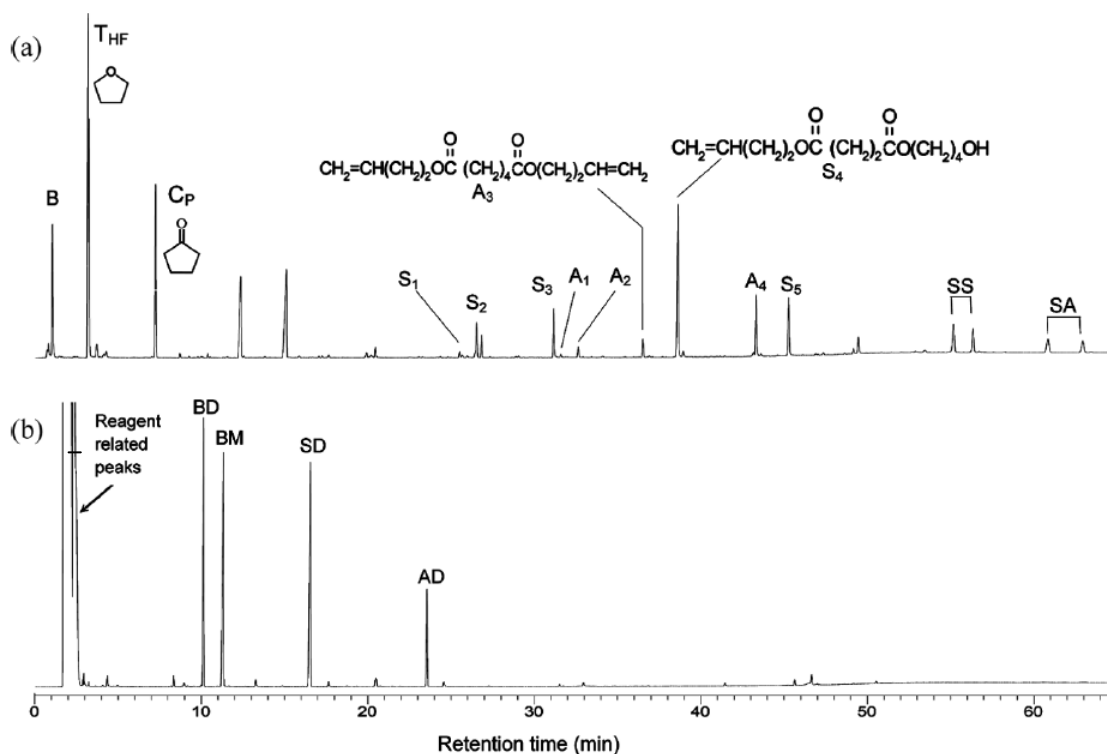


Figure 2.7 : Pyrograms of reactive Py-GC products from original P(BS-*co*-BA) film sample obtained (a) without TMAH at 500°C and (b) in the presence of TMAH at 350°C. Peak assignment of pyrogram (a) : B = butane, T_{HF} = tetrahydrofuran, C_P = cyclopentanone, S_x = ester compound with a succinate unit, A_x = ester compound with an adipate unit, SS = succinate dimers, SA = hybrid dimmers of succinate and adipate units. The abbreviations are shown in Table 2.1.

Table 2.1 : Identification of the characteristic peaks on the pyrograms obtained by reactive Py-GC of P(BS-*co*-BA) in the presence of TMAH.

Peak	Structure	MW	ECN ^a
Butanediol dimethyl ether (BD)	$\text{H}_3\text{C}-\text{O}-\left(\text{CH}_2\right)_4-\text{O}-\text{CH}_3$	118	4.4
Butanediol monomethyl ether (BM)	$\text{HO}-\left(\text{CH}_2\right)_4-\text{O}-\text{CH}_3$	120	6.4
Succinic acid dimethyl (SD)	$\text{H}_3\text{C}-\text{O}-\overset{\text{O}}{\parallel}{\text{C}}-\left(\text{CH}_2\right)_2-\overset{\text{O}}{\parallel}{\text{C}}-\text{O}-\text{CH}_3$	146	3.5
Adipic acid dimethyl (AD)	$\text{H}_3\text{C}-\text{O}-\overset{\text{O}}{\parallel}{\text{C}}-\left(\text{CH}_2\right)_4-\overset{\text{O}}{\parallel}{\text{C}}-\text{O}-\text{CH}_3$	174	5.5

^a The effective carbon number

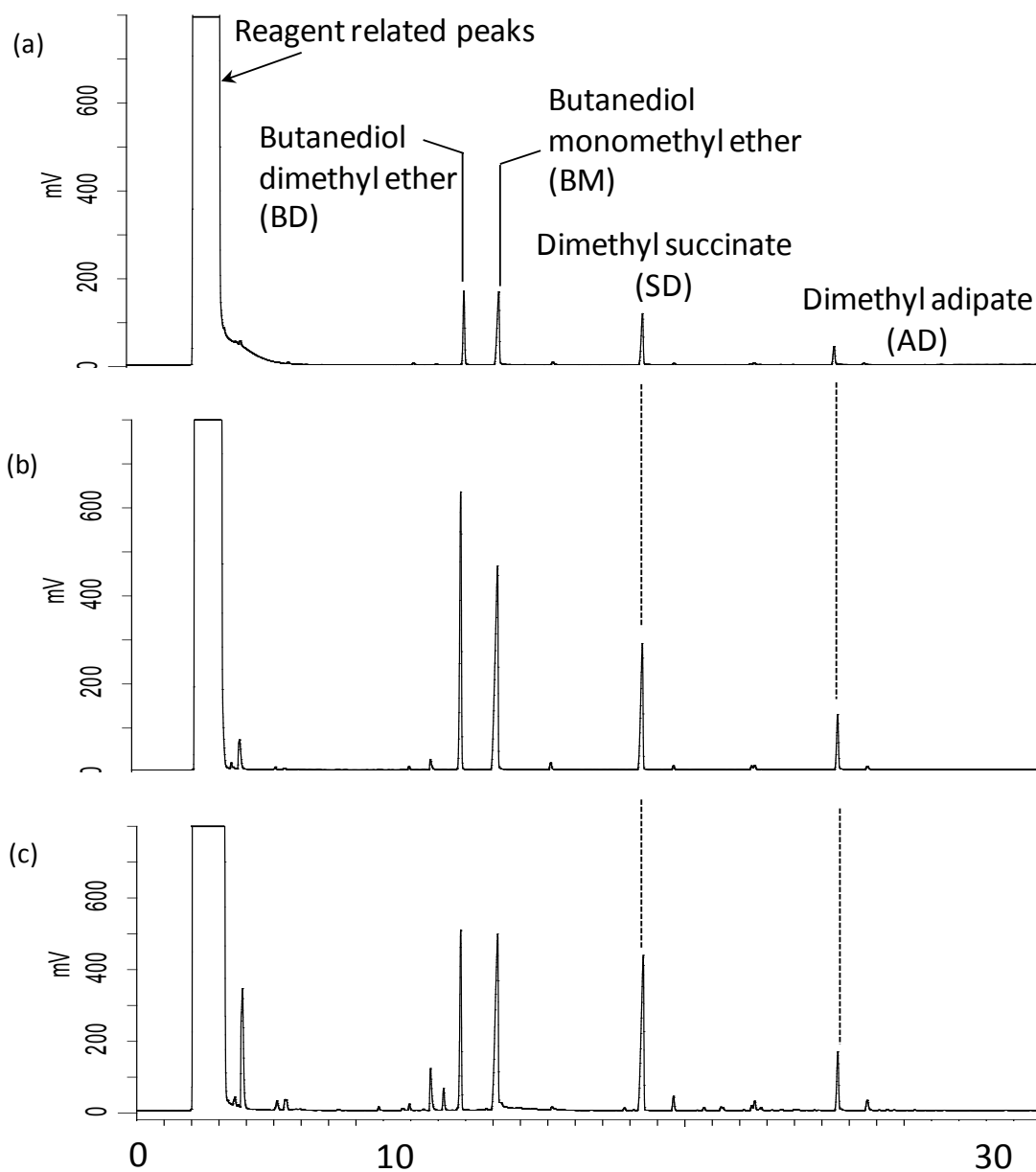


Figure 2.8 : Typical pyrograms of P(BS-*co*-BA) film samples (50 μ g) obtained by reactive Py-GC in the presence of TMAH at : (a) 300°C, (b) 350°C, and (c) 500°C.

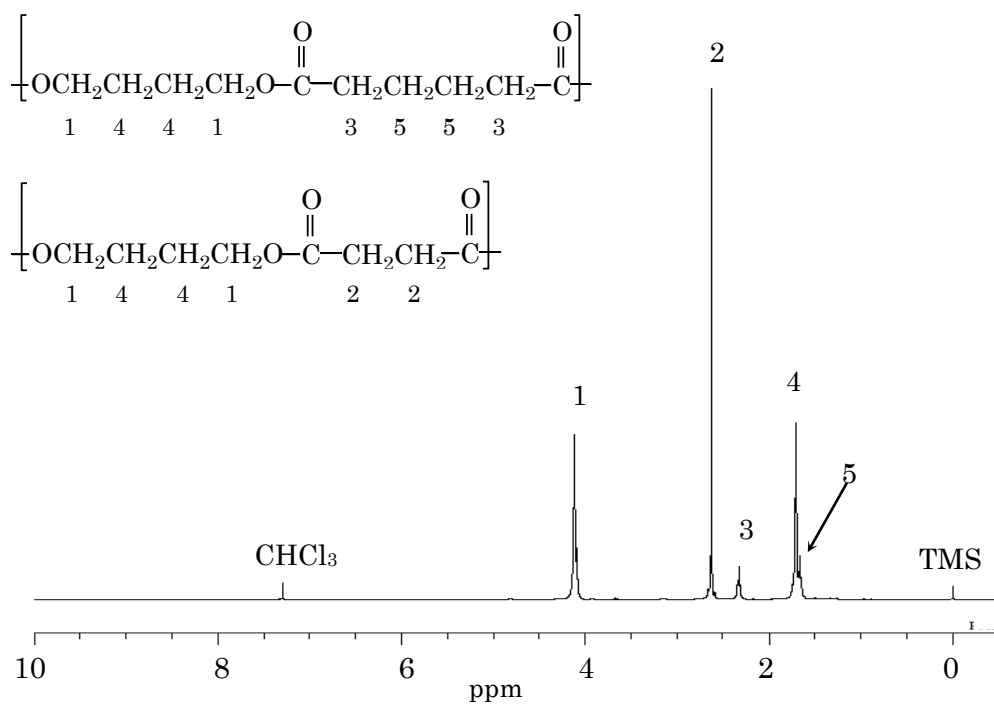


Figure 2.9 : $^1\text{H-NMR}$ spectrum of original P(BS-*co*-BA) film sample without biodegradation. Peak assignment: 1 and 4 derived from methylene protons of 1,4-butanediol unit, 2 from methylene protons of succinate unit, 3 and 5 from methylene protons of adipate unit.

2.3.2 Reactive Py-GC of P(BS-*co*-BA) Samples after Soil Burial Degradation Test

Figure 2.10 shows the pyrograms of the P(BS-*co*-BA) samples prepared by homogenized in chloroform solutions of (a) control P(BS-*co*-BA) and (b) the film recovered after soil burial for 28 days. Although the relative peak intensities of BD and BM differed between these two pyrograms, the ratios of the two peaks were not repeatable for each measurement because of the lower reactivity of butanediol moieties in P(BS-*co*-BA) with TMAH owing to their lower polarity. Meanwhile, it is interesting to note that the relative peak intensities of SD slightly increase while those of AD decrease after soil burial. Because this tendency is reproducibly observed, it is suggested that the BA moieties preferentially decompose during the burial degradation test. Subsequently, the changes in the copolymer compositions between BS and BA in P(BS-*co*-BA) with the elapsed time of the soil burial test were examined in detail in order to investigate the biodegradation behaviors of the P(BS-*co*-BA) samples.

Table 2.2 shows the changes in the average copolymer composition of BS and BA moieties during the soil burial test, calculated from the peak intensities of SD and AD on the pyrograms of the P(BS-*co*-BA) solution samples according to Eqs. (1) and (2), together with the recovery (wt.%). As shown in this table, the copolymer compositions of BS gradually increased, while that of BA decreased with soil burial time, almost correlating with the decrease in recovery. Here, the changes in copolymer compositions can be explained by considering the effect of crystallinity of the P(BS-*co*-BA) sample on its biodegradation. It is known that the BA moieties in the polymer chains preferentially biodegrade due to their relatively lower crystallinity,^{4,11} which in turn results in decreased compositions of BA for the recovered film samples.

This observation suggests that the copolymer compositions determined by reactive Py-GC can be used as a good measure to evaluate the degree of biodegradation of P(BS-*co*-BA).

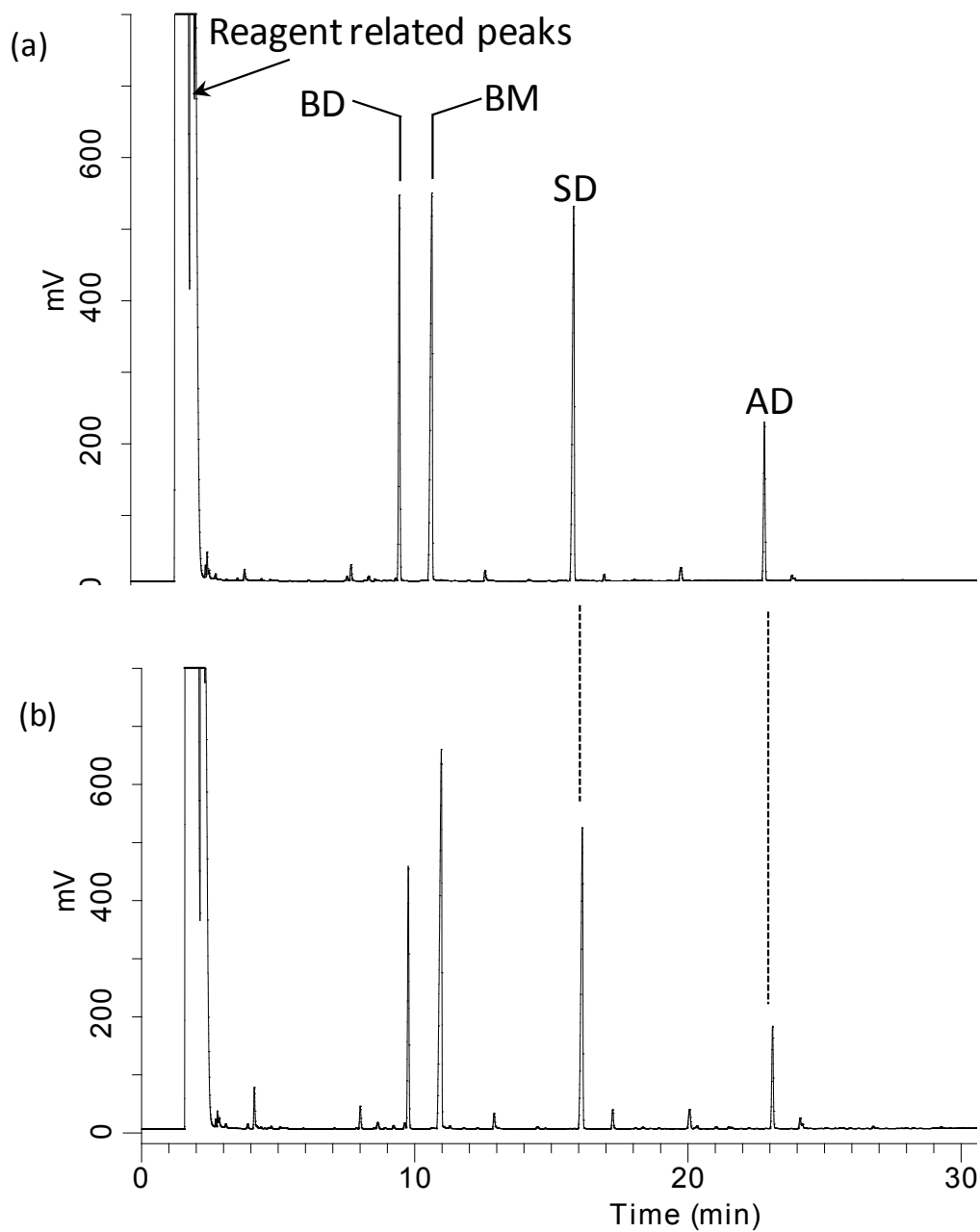


Figure 2.10 : Pyrograms of P (BS-co-BA) solution sample by reactive Py-GC at 350°C; (a) before and (b) after 4 weeks of soil burial degradation test. The abbreviations are shown in Table 2.1.

Table 2.2 : Changes in average copolymer composition of P(BS-*co*-BA) film during soil burial degradation test determined by reactive Py-GC.

Degradation Time (days)	Copolymer composition (%) BS : BA	Recovery (wt %)
Original	82.2 : 17.8 ^a (80.0 : 20.0) ^b	100
7	82.8 : 17.2	97.2
14	83.0 : 17.0	92.4
21	84.1 : 15.9	78.0
28	85.5 : 14.5	68.1

^a RSD = Less than 1 % ($n = 5$).

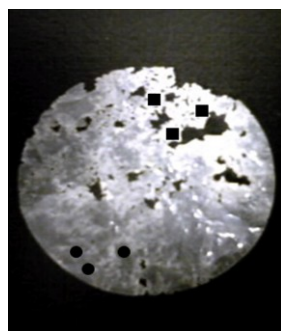
^b Reference value obtained by ¹H-NMR.

2.3.3 Local Biodegradation in P(BS-*co*-BA) Film Samples Evaluated By Reactive Py-GC

Finally, local biodegradation in a degraded P(BS-*co*-BA) film sample was studied. In this case, the degree of biodegradation at a local point in a given film sample was evaluated based on the copolymer compositions determined by reactive Py-GC using only trace amounts (approximately 20 μg) of the sample. Table 2.3 shows the copolymer compositions estimated for various sampling spots by reactive Py-GC in a biodegraded P(BS-*co*-BA) film sample recovered after three weeks of soil burial, together with a photograph of the recovered film designating the sampling points. The photograph demonstrates that the degraded film became fairly opaque, with many holes formed through erosion by microorganisms, although transparent parts can be still observed, mainly at the edge of the film. Here, the average copolymer compositions shown in this table were in disagreement with the value after three weeks of soil burial in Table 2.2 since these two burial tests were carried out at different seasons, which led to a change in the concentration of microorganisms in the soil. As shown in this table, the copolymer compositions of BA moiety remained almost the same as that for the original film sample at transparent spots, while the corresponding values at opaque spots were slightly lower than those at transparent spots. This observation reflects that biodegradation of the BA moieties preferentially occurred at opaque spots. These results demonstrate that reactive Py-GC can be a promising technique to elucidate the local variation of biodegradation in a given biodegraded film sample.

Table 2.3 : Local copolymer compositions estimated by reactive Py-GC for biodegraded P(BS-*co*-BA) film sample recovered after soil burial for three weeks.

Sampling spot		BS %	BA %
Transparent spots (●)	# 1	82.2	17.8
	# 2	82.3	17.7
	# 3	82.2	17.8
Mean		82.2	17.8
Opaque spots (■)	# 1	83.7	16.3
	# 2	83.6	16.4
	# 3	83.5	16.5
Mean		83.6	16.4
Average value of whole film sample		82.9	17.1



2.4 Conclusions

Reactive Py-GC proved to be a rapid and highly sensitive method to determine copolymer composition of biodegradable P(BS-*co*-BA) without using any tedious sample pretreatment. Taking advantage of the fact that this technique requires only trace amounts (approximately 20 μg) of the sample, evaluation of local degradation for a given degraded P(BS-*co*-BA) film was successfully carried out on the basis of variations in the observed copolymer compositions. This method can be applied to elucidate the degree of local biodegradation for P(BS-*co*-BA) products widely used as casting films and sheet extrusions.

References

1. R. Ishioka, E. Kitakuni, and Y. Ichikawa, in “Biopolymers Online”, A. Steinbuechel ed., Wiley-VCH Verlag GmbH & Co. KGaA, p.275-297, 2005 (10. Aliphatic Polyesters : Bionolle).
2. T. Uesaka, K. Nakane, S. Maeda, T. Ogihara, and N. Ogata, *Polymer*, **41**, 8449–8454 (2000).
3. T. Fujimaki, *Polym. Degrad. Stab.* **59**, 209–214 (1997).
4. S. S. Ray, J. Bandyopadhyay, and M. Bousmina, *Polym. Degrad. Stab.*, **92**, 802–812 (2007).
5. V. Tserki, P. Matzinos, E. Pavlidou, D. Vachliotis, and C. Panayiotou, *Polym. Degrad. Stab.*, **91**, 367–376 (2005).
6. V. Tserki, P. Matzinos, E. Pavlidou, D. Vachliotis, and C. Panayiotou, *Polym. Degrad. Stab.* **91**, 377–384 (2006).
7. Kuraoka, K., N. Soshi, and N. Kawasaki, *J. Polym. Res.*, **18**, 279–282 (2010).
8. A. Lindstrom, A.-C. Albertsson, and M. Hakkarainen, *Polym. Degrad. Stab.* **83**, 487–493 (2004).
9. H. Sato, M. Furuhashi, D. Yang, H. Ohtani, S. Tsuge, M. Okada, K. Tsunoda, and K. Aoi, *Polym. Degrad. Stab.*, **73**, 327–334 (2001).
10. A. D. Jorgensen, K. C. Picel, and V. C. Stamoudis, *J. Anal. Chem.* **62**, 683–689 (1990).
11. M. S. Nikolic and J. Djonlagic, *Polym. Degrad. Stab.*, **74**, 263–270 (2001).

Chapter 3

Evaluation of Biodegradation Behavior of Poly(butylene succinate-*co*-butylene adipate) with Lowered Crystallinity by Reactive Pyrolysis-Gas Chromatography

3.1 Introduction

In Chapter 2, reactive Py-GC was successfully applied to the compositional analysis of poly(butylene succinate-*co*-butylene adipate) [P(BS-*co*-BA)] before and after the biodegradation only using trace amounts (ca. 20 µg) of the film samples.¹ The copolymer compositions of the P(BS-*co*-BA) samples were rapidly and precisely determined from the peak intensities of dimethyl succinate and dimethyl adipate derived from the butylene succinate (BS) and butylene adipate (BA) units, respectively, in the polymer chains through the reactive pyrolysis. Furthermore, it was revealed that the BA content in the film samples gradually decreased with soil burial degradation time, reflecting preferential biodegradation of the BA-rich moieties with the elapsed time of soil burial. Although the reason for this change in copolymer composition during soil burial was not experimentally unraveled, local differences in biodegradability of a given P(BS-*co*-BA) film after soil burial were analyzed in detail based on the observed compositions.¹

Here, we presumed that the preferential degradation of the BA rich moieties during soil burial might be explained by considering the effect of crystallinity of the P(BS-*co*-BA) sample on its biodegradation. So far, some researchers have attempted to evaluate the influence of crystallinity upon the biodegradation behavior of P(BS-*co*-BA), focusing on the chemical structure and copolymer composition.²⁻⁶ Tserki et al.^{4,5} reported that the degree of crystallinity was lowered by introducing BA units into a BS homopolymer, and became the lowest when the composition between the butylene succinate (BS) and the butylene adipate (BA) units was 40/60. Moreover, it was revealed that the highest enzymatic degradation rates was also observed at the copolymer composition of BS/BA = 40/60, reflecting the lowest degree of crystallinity.

Ahn et al. examined the biodegradability for BS and BA homopolymers and a series of P(BS-*co*-BA) copolymers with the BA content from 10 to 90% in the composting soils. As a result, biodegradability of the P(BS-*co*-BA) samples in the soils increased as the BA content in the copolymers increased from 10 to 60% because of the lowering of crystallinity.³

These studies mentioned above suggest that the difference in crystallinity between the BS- and BA-rich moieties in the copolymer chains played an important role for the change in copolymer composition during biodegradation observed in Chapter 2. The copolymer chains containing large amount of the BA units could show relatively lower crystallinity than the BS-rich chains. This feature in turn should lead to preferential biodegradation of the BA-rich moieties although the BS-rich chains must be hardly degraded because of their highly crystalline nature. One of the approaches to prove this assumption is to subject a P(BS-*co*-BA) film with lowered crystallinity even for the BS-rich moieties to the soil burial test, and trace the change in the copolymer composition during biodegradation. If the hypothesis is correct, the change in the copolymer composition is to be relatively small compared to the original P(BS-*co*-BA) film.

In this study, we tried to evaluate the biodegradation behaviour of P(BS-*co*-BA) samples with lowered degree of crystallinity by means of reactive Py-GC in order to clarify the reason for preferential degradation of the BA-rich moieties in original P(BS-*co*-BA) films during soil burial. Commercially available P(BS-*co*-BA) film samples and those with lower degree of crystallinity, prepared by heating and cooling quickly the original P(BS-*co*-BA) films, were subjected to a soil burial biodegradation test. Various stages of the degraded film samples were then analyzed by reactive

Py-GC in order to trace the change in the copolymer composition during the soil burial test. The observed difference in the change of the composition between the original and heated films was interpreted in terms of the biodegradation behavior of these P(BS-*co*-BA) films with the observed weight loss during biodegradation.

3.2 Experimental

3.2.1 Materials

The film samples of commercially available P(BS-*co*-BA) (Bionolle 3001, Showa Denko Co. Ltd., Japan) were used in this work. A small amount (approximately 0.5%) of hexamethyl diisocyanate units was introduced into the P(BS-*co*-BA) sample in order to elongate the polymer chains. The film samples with lower degree of crystallinity were prepared by heating the original ones at 80 °C for 20 min and subsequently cooling them quickly in ice water.

3.2.2 Soil Burial Biodegradation Test

A soil burial degradation test of the original and heated P(BS-*co*-BA) films was carried out according to the procedure described in Chapter 2. Circular pieces (approximately 15 mg) of thin P(BS-*co*-BA) films (30 mm diameter, 35 μm thickness) were subjected to a soil burial biodegradation test for 1-4 weeks. The soil (pH 5.3) used in this study had been composted in the farm at Chubu University (Kasugai, Aichi Prefecture, Japan) and was contained in a small box in an incubator, in which the relative humidity was adjusted to approximately 90% and the temperature was kept constant at 30 °C. After designated periods, each degraded P(BS-*co*-BA) film was washed with water, dried, and weighed. The weight loss (weight %) of each degraded film was calculated from its dry weight normalized by that of the film sample before the burial test.

3.2.3. Differential Scanning Calorimetry (DSC) measurement

The DSC scans were recorded using a Bruker AXS DSC 3100 analyzer. About 10 mg of P(BS-*co*-BA) film samples was heated under a nitrogen flow of 20 ml/min. The temperature was programmed from 35°C to 150°C at a heating rate of 10°C/min.

3.2.4 Reactive Py-GC Measurement

The reactive Py-GC system used in this study was basically the same as that described in Chapter 2. A microfurnace pyrolyzer (Frontier laboratories, PY-2010D) was attached to a GC (Agilent, HP 4890) equipped with a flame ionization detector (FID). The small platinum cup (2 mm i.d. × 4 mm height) containing 2 µl of the chloroform solution (10 mg/ml) of each film sample together with 2 µl TMAH solution (2.2 M in methanol, Aldrich) was dropped in the center of a pyrolyzer heated at 350°C under a helium carrier gas flow (50 ml/min). A part of the flow (1 ml/min) reduced by a splitter was introduced into a metal capillary separation column (Frontier Laboratories, Ultra ALLOY-5 (MS/HT); (30 m long × 0.25 mm i.d.) coated with immobilized 5% diphenyl-95% dimethylpolysiloxane (1.0 µm film thickness). The column temperature was programmed from 50°C to 300°C at a rate of 5°C/min. Identification of the peaks on the chromatograms was carried out by using a reactive Py-GC-mass spectrometry (MS) system (Shimadzu, QP-5050 with an electron ionization (EI) sources).

3.3 Results and Discussion

Figure 3.1 shows the DSC thermograms of (a) the original and (b) heated P(BS-*co*-BA) film samples before biodegradation test. From the areas of melting endothermic peaks observed in these thermograms, the measured values of the heat of fusion were estimated at 53.0 and 48.6 J/g for the original and heated film samples, respectively. Then, the degree of crystallinity of P(BS-*co*-BA) can be calculated from the measured value of the heat of fusion divided by the theoretical value for the 100% crystalline copolyester according to the method reported by Tserki et al.^{4,5} The obtained degree of crystallinity for the original and heated film samples were 46.1 and 42.4%, respectively, indicating that crystallinity of the P(BS-*co*-BA) film was considerably lowered by heat and cool treatment.

Figure 3.2 shows the pyrograms of (a) the original and (b) heated P(BS-*co*-BA) films samples before the biodegradation test obtained by reactive Py-GC at 350 °C. As was reported in Chapter 2, four main peaks, butanediol dimethyl ether (BD), butanediol monomethyl ether (BM), dimethyl succinate (SD), and dimethyl adipate (AD), were mainly observed after the elution of TMAH-related products on these two chromatograms.¹ These peaks were formed partially through selective hydrolysis of ester linkages in the polymer chains followed by simultaneous methylation. In addition, some of the other small peaks appearing in the chromatograms might be derived from the hexamethylene diisocyanate units introduced into the P(BS-*co*-BA) chains.

From the peak areas of SD and AD, the copolymer compositions of the BS and BA units in the P(BS-*co*-BA) samples, C_{BS} and C_{BA} (mol%) were calculated by the following equations, as proposed in Chapter 2 :

$$C_{BS} \text{ (mol \%)} = [(P_{SD} / 3.5) / \{P_{SD} / 3.5\} + (P_{AD} / 5.5)\}] \times 100 \quad (1)$$

$$C_{BA} \text{ (mol \%)} = [(P_{AD} / 5.5) / \{P_{SD} / 3.5\} + (P_{AD} / 5.5)\}] \times 100 \quad (2)$$

where P_{SD} and P_{AD} are observed peak intensities of SD and AD, respectively. The values of 3.5 and 5.5 are the calculated response for FID (effective carbon number) of SD and AD, respectively. It is interesting to note that the copolymer composition (BS/BA) for the two samples calculated from Eqs. (1) and (2) showed almost same values; 82.2/17.8 and 82.6/17.4 for the original and the heated film, respectively. The relative standard deviations for the observed copolymer compositions were less than 5% for three repeated reactive Py-GC measurements. These results indicate that the reaction efficiency of TMAH with P(BS-*co*-BA) during reactive Py-GC measurement is not affected by its crystallinity, thus reactive Py-GC enables to analyze the copolymer compositions of the P(BS-*co*-BA) samples with sufficient precision and accuracy independent of the degree of crystallinity.

The change in copolymer composition of P(BS-*co*-BA) during the soil burial test was then determined by reactive Py-GC both for the original and heated film samples. Table 3.1 summarizes the observed copolymer compositions of the P(BS-*co*-BA) film samples subjected to various degrees of biodegradation with the weight loss (wt.%) both for the heated and original films. The data for the original P(BS-*co*-BA) samples were the same as those reported previously in Chapter 2. The weight loss for the heated film samples was much higher than those for the original ones.

For example, the weight loss for the original and heated film samples after the soil burial test for 4 weeks were determined to be 31.9 and 85.6 wt%, respectively. This fact demonstrates that the biodegradation rate was highly promoted for the heated P(BS-*co*-BA) film samples. On the other hand, as was expected from the assumption described earlier, the decreases in the BA content during soil burial were slightly smaller for the heated film samples compared to the original ones. For example, the BA contents after 28 days of the soil burial test for the original and heated film samples were estimated to be 14.5 and 15.9%, respectively.

Figure 3.3 illustrates possible biodegradation models of the P(BS-*co*-BA) samples estimated from the observed weight losses and the change in the copolymer compositions shown in Table 3.1. As for the original P(BS-*co*-BA) films, as was previously supposed, the BA-rich moieties could show relatively lower crystallinity than the BS-rich moieties, which in turn should lead to preferential biodegradation of the BA-rich moieties as illustrated in Figure 3.3 (a). In this case, the BA content is to be decreased with the elapsed time of biodegradation as observed in Chapter 2.

As for the heated film samples, the changes in the copolymer composition during biodegradation were relatively small, while much larger weight loss was observed compared to the original film samples. In these film samples, crystallinity would be considerably lowered even for the BS-rich polymer chains by heating and cooling quickly the films. In this case, biodegradation could be promoted and proceed with the comparable rate both for the BA and BS-rich moieties, which lead to much higher degradability of the heated film samples with the smaller change in the copolymer composition as shown in Figure 3.3 (b).

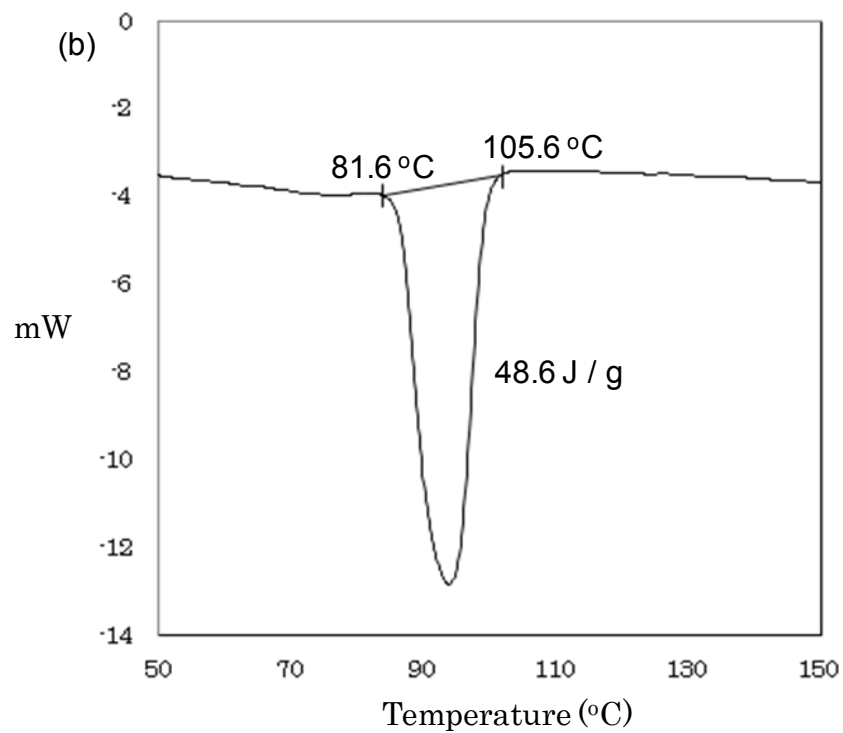
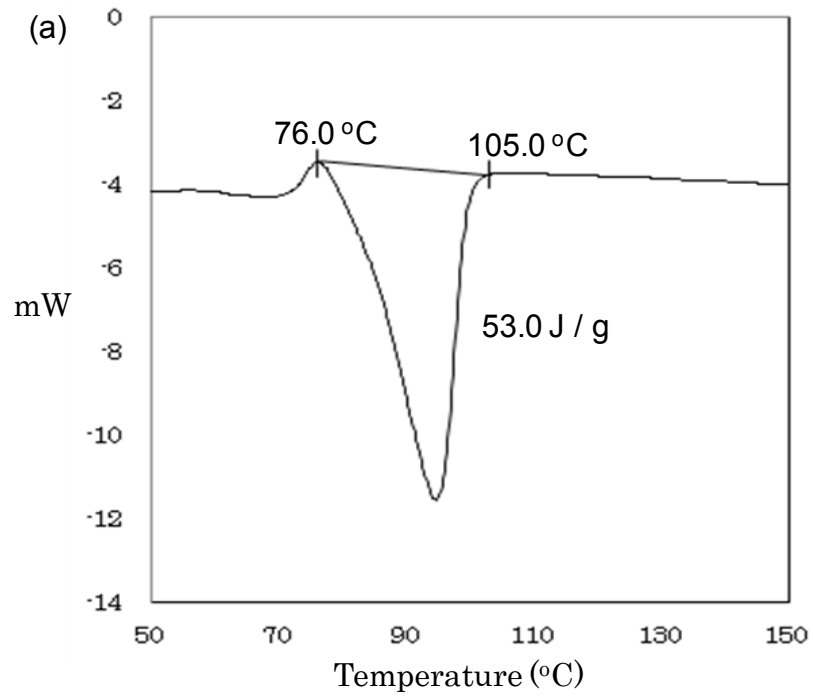


Figure 3.1 : DSC thermograms of P(BS-*co*-BA) film samples without biodegradation :
(a) original film sample and (b) heated film.

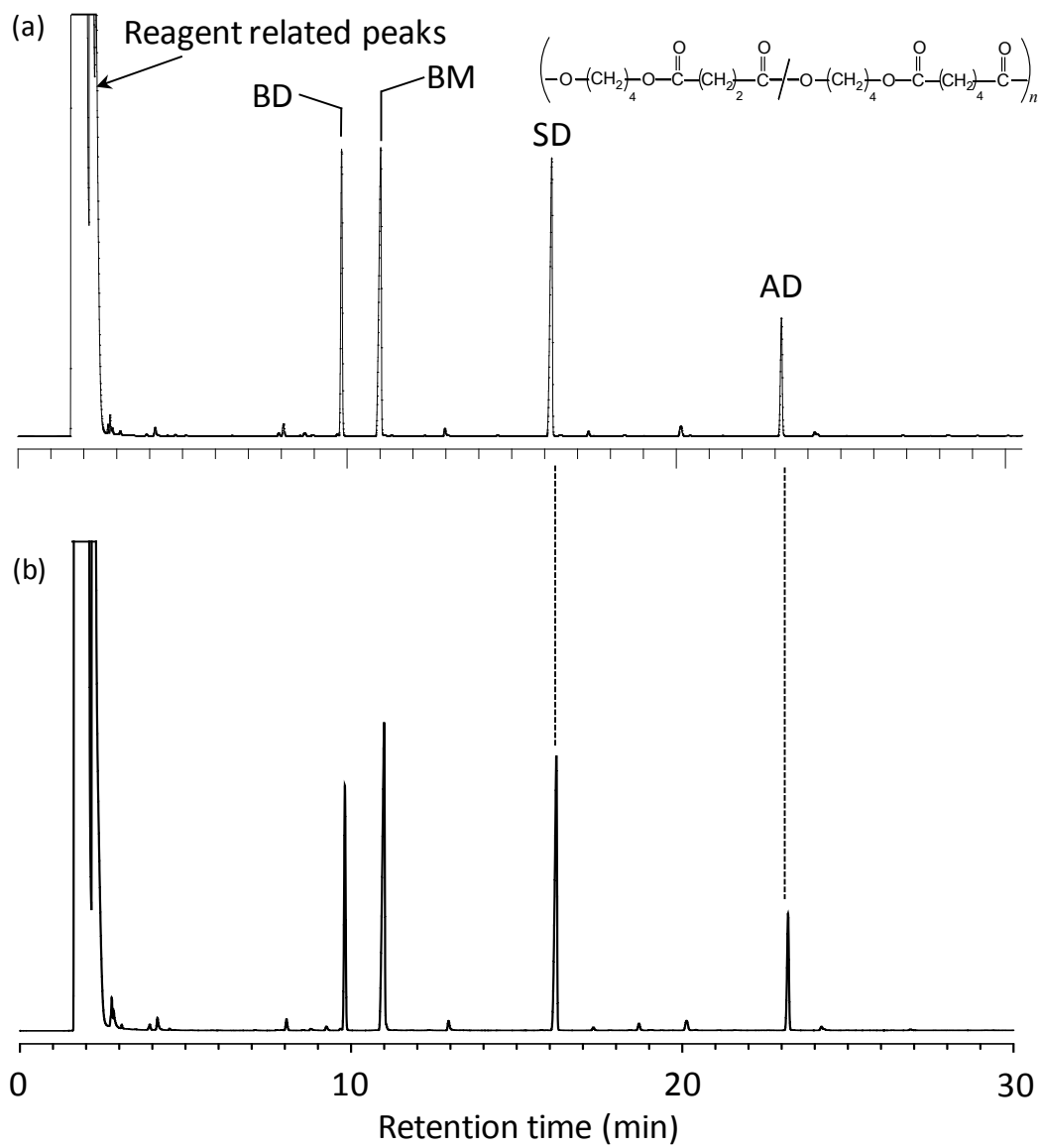


Figure 3.2 : Pyrograms of P(BS-co-BA) film samples without biodegradation obtained by reactive Py-GC at 350°C: (a) original film (b) heated film.

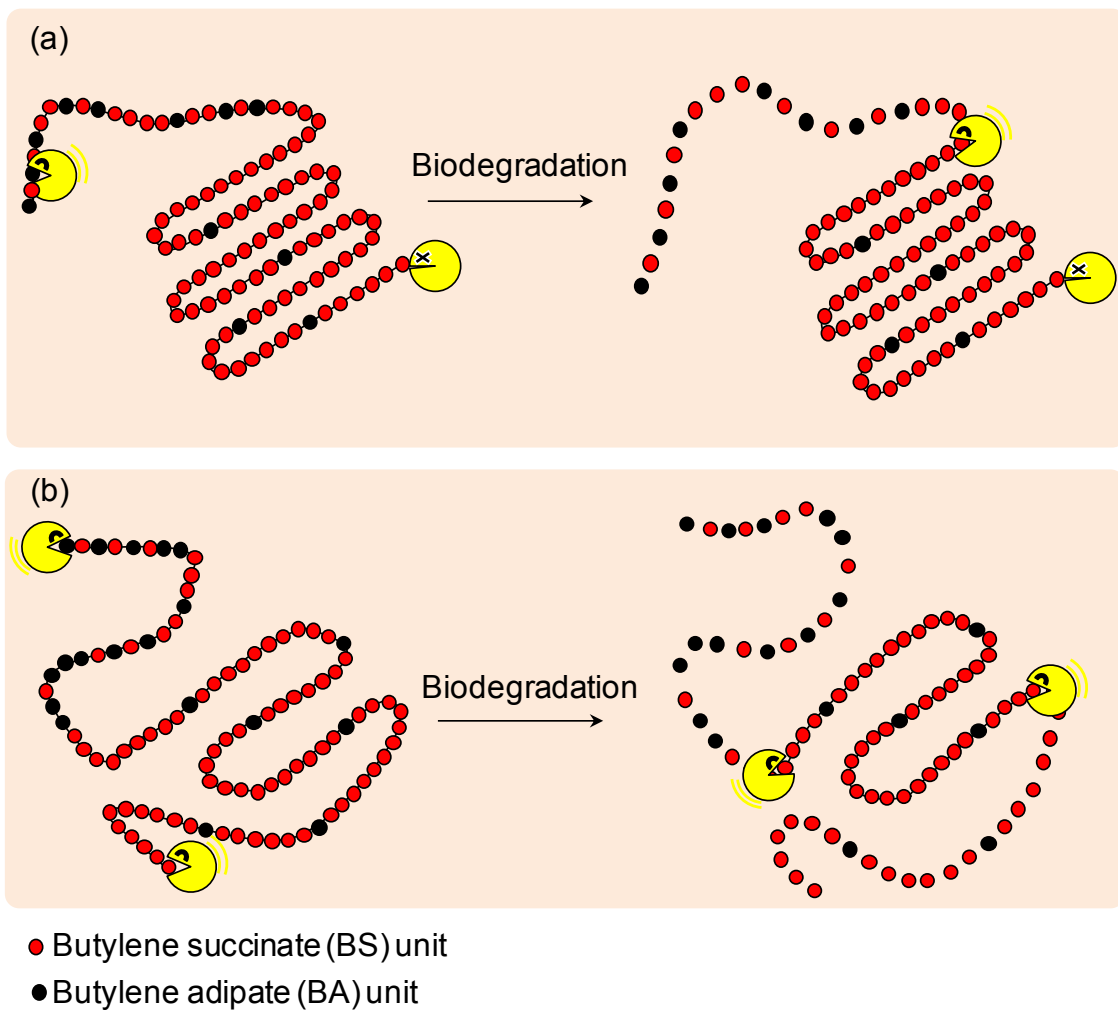


Figure 3.3 : Possible biodegradation models of (a) original and (b) heated P(BS-*co*-BA) film samples.

Table 3.1 : Changes in copolymer compositions of original and heated P(BS-*co*-BA) film samples during soil burial degradation test determined by reactive Py-GC with weight loss.

Degradation time (days)	Heated films		Original Films ¹	
	Weight loss (%)	Composition (mol%) BS : BA	Weight loss (%)	Composition (mol%) BS : BA
0	0	82.6 : 17.4 ^a	0	82.2 : 17.8
7	3.2	83.3 : 16.7	2.8	82.8 : 17.2
8	9.4	83.4 : 16.6	-	-
10	11.6	83.6 : 16.4	-	-
14	31.3	83.7 : 16.3	7.6	83.0 : 17.0
21	55.6	84.3 : 15.7	22.0	84.1 : 15.9
28	85.6	84.1 : 15.9	31.9	85.5 : 14.5

^a RSD = less than 5 % ($n = 3$)

3.4 Conclusions

The biodegradation behavior of P(BS-*co*-BA) films with lowered crystallinity by heating and quickly cooling the original films was studied by reactive Py-GC in the presence of TMAH. As a result, the change in the copolymer composition during a soil burial test observed by reactive Py-GC was relatively smaller for the heated P(BS-*co*-BA) films than that of the original ones. Furthermore, the biodegradation rate was highly promoted compared to the original films owing to the lowered crystallinity. These results suggest that biodegradation was promoted and proceeded with the comparable rate both for the BA and BS-rich moieties in the heated films. Taking these features into consideration, the reason for the change in copolymer composition observed for the original P(BS-*co*-BA) films can be clarified as follows:

- (1) the BA-rich moieties in the copolymer chains could show relatively lower crystallinity than the BS-rich moieties.
- (2) the BA-rich moieties were preferentially biodegraded during soil burial test, leading to the decreased BA content as the biodegradation proceeded.

References

1. S. Baidurah, S. Takada, K. Shimizu, K. Yasue, S. Arimoto, Y. Ishida, T. Yamane, and H. Ohtani, *Int. J. Polym. Anal. Ch.*, **17**, 29–37 (2012).
2. G. Montaudo and P. Rizzarelli, *Polym. Degrad. Stab.*, **70**, 305–314 (2000).
3. B.D. Ahn, S.H. Kim, Y.H. Kim, and J.S. Yang, *J. Appl. Polym. Sci.*, **82**, 2808–2826 (2001).
4. V. Tserki, P. Matzinos, E. Pavlidou, D. Vachliotis, and C. Panayiotou, *Polym. Degrad. Stab.*, **91**, 367–376 (2006).
5. V. Tserki, P. Matzinos, E. Pavlidou, and C. Panayiotou, *Polym. Degrad. Stab.*, **91**, 377–384 (2006).
6. M.S. Nikolic and J. Djonlagic, *Polym. Degrad. Stab.*, **74**, 263–270 (2001).

Chapter 4

Rapid and Direct Compositional Analysis of Poly(3-hydroxybutyrate-*co*-3-hydroxyvalerate) in Whole Bacterial Cells by Reactive Pyrolysis-Gas Chromatography

4.1 Introduction

Poly(3-hydroxybutyrate-*co*-3-hydroxyvalerate), [P(3HB-*co*-3HV)] (Figure 4.1) is one of the biodegradable copolyesters produced by several species of bacteria, such as *Cupriavidus necator* and *Bacillus megaterium*, as energy storage compounds in their cells. It has been reported that the amount of P(3HB-*co*-3HV) accumulated in the cells changes drastically depending on the species of bacteria and the culture conditions. *C. necator* has been known to accumulate a large amount of P(3HB-*co*-3HV) when the carbon source in growth medium is rich but the nitrogen source is limited.¹⁻³ Moreover, the addition of propionic acid or valeric acid to the growth media leads to the production of a random copolymer composed of 3HB and 3HV units.

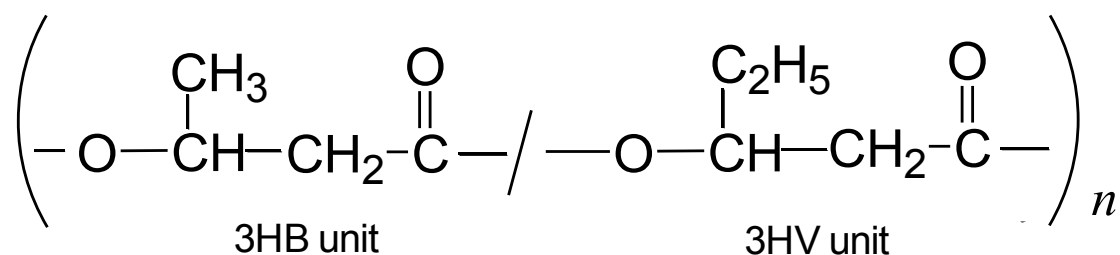


Figure 4.1 : Chemical structure of P(3HB-*co*-3HV)

P(3HB-*co*-3HV) has been widely used as compost bags and packaging materials due to its excellent physical and chemical properties, and non-toxic behavior.^{1,4-6} It is well known that the copolymer composition of P(3HB-*co*-3HV) is closely related to its physical properties such as transparency, degree of crystallinity and

the rate of biodegradation.⁷ Furthermore, the data concerning the copolymer composition might provide a clue to elucidate the biodegradation mechanism of the polymer chains.⁸ Therefore, in order to determine the species of bacteria and the culture conditions suited for the production of P(3HB-*co*-3HV) with high performances, it is necessary to develop a practical and highly sensitive method to analyze the copolymer composition of the copolyester accumulated in the whole cells.

In general, the copolymer composition of P(3HB-*co*-3HV) in bacterial cells has been analyzed by means of gas chromatography (GC) following preliminary sample treatments such as trans-esterification and solvent extraction.⁹⁻¹⁴ Rao et al.¹⁴ have used GC to determine the content and composition of P(3HB-*co*-3HV) in the lyophilized cells of *C. necator*. Approximately 15 mg of the lyophilized cells were subjected to methanolysis in the presence of methanol and sulfuric acid [85% : 15% (v/v)] at 100°C for three hours. Then the organic layer containing the reaction products was separated, dried over Na₂SO₄, and analyzed by GC. Based on the peak intensities of methylated monomer components on the pyrograms, the content and the composition of the P(3HB-*co*-3HV) were 85 mol% 3HB and 15 mol% 4HB. This technique, however, required a fairly large amount of sample (at least 20 mg) and a relatively long sample pretreatment time (approximately half a day) prior to a final GC measurement.

To shorten the sample pretreatment time, Betancourt *et al.* developed a rapid microwave assisted esterification technique for the analysis of P(3HB) in bacteria by GC.¹³ In this technique, the lyophilized bacterial biomass was directly subjected to microwave irradiation in acidic methanol to esterify P(3HB) rapidly in the whole cells. By using this technique, they drastically reduced the time required for the esterification process of P(3HB) to 4 minutes. This method, however, was not always applied to

routine analyses because a relatively large amount of sample (at least a few mg) was still needed for the sample pretreatment.

Recently, reactive Pyrolysis-Gas Chromatography (reactive Py-GC) in the presence of tetramethylammonium hydroxide (TMAH) was used to determine the copolymer composition of trace amounts (ca. 0.1 mg or less) of isolated P(3HB-*co*-3HV).¹⁵ It was revealed that P(3HB-*co*-3HV) subjected to pyrolysis in the presence of TMAH around 350°C underwent not only the typical pyrolysis reaction but also *cis*-elimination of the ester linkages followed by hydrolysis and methylation of the adjacent ester bond. Based on the peak intensities of the products formed from these reactions, the copolymer compositions were analyzed precisely and accurately without using any cumbersome pretreatment.

In this study, reactive Py-GC was applied to rapid and direct analysis of copolymer compositions for P(3HB-*co*-3HV) accumulated in bacteria. First, bacterial cells containing P(3HB-*co*-3HV) with various copolymer compositions were cultured, and were directly subjected to reactive Py-GC measurements without any sample pretreatment. Then for the sake of validating of the reactive Py-GC method, the measured copolymer compositions of P(3HB-*co*-3HV) in bacteria were compared to those by the conventional method involving off-line trans-methylation and solvent extraction.

4.2 Experimental

4.2.1 Materials

C. necator NBRC 102504 which was purchased from NITE Biological Resources Center (NBRC, Japan) was used since the species had been extensively studied for the production of P(3HB-*co*-3HV).² The industrially available P(3HB-*co*-3HV) (Mitsubishi Gas Chemical Co., Inc., Japan) with 15 mol% 3HB and 85 mol% 3HV contents, in the form of fine powders was also utilized. A methanol solution of tetramethylammonium hydroxide (TMAH) (2.2 M) was purchased from Aldrich (Milwaukee, WI). In addition, methanol containing 10% v/v of H₂SO₄ supplied from Supelco Inc. (Bellefonte, PA) was also used for the trans-methylation of P(3HB-*co*-3HV) in the conventional method.

4.2.2 Culture conditions of *C. necator* for P(3HB-*co*-3HV) copolymer production

C. necator cells were cultured in a two-stage process as shown in Figure 4.2. In the first stage, glucose was used as a sole carbon source in order to encourage cell proliferation. According to a report by Chandprateep et al.,¹⁶ the medium was composed of 10 g/l glucose, 5.8 g/l K₂HPO₄, 3.7 g/l KH₂PO₄, 0.5 g/l (NH₄)₂SO₄, 0.12 g/l MgSO₄·7H₂O, and 1 ml of a solution of trace elements (1.67 g/l CaCl₂·2H₂O, 2.78 g/l ZnSO₄·7H₂O, 0.29 g/l FeSO₄·7H₂O, 1.98 g/l MnCl₂·4H₂O, 0.17 g/l CuCl₂·2H₂O). The bacteria in 200 ml of the culture volume were incubated in a rotary shaker (55 rpm) for 48 hours at 30°C. The cells were harvested by centrifugation, and then transferred to a nitrogen-limiting medium containing valeric acid as a sole carbon source to promote P(3HB-*co*-3HV) accumulation. In this second stage, the medium was

prepared as follows based on the report by Abdelhad et al.,¹⁷ the medium was composed of 0.56, 0.28 and 0.14 g/l Valeric acid, 4.0 g/l (NH₄)₂SO₄, 13.3 g/l KH₂PO₄, 1.7 g/l citric acid, 1.2 g/l MgSO₄·7H₂O, and 1 ml of the same solution of trace elements as that in the initial stage. The culture volume and pH of the medium were set at 200 ml and 6.8, respectively. Here, the molar ratio of valeric acid, added in the medium at the second stage, to glucose (V/G) added at the first stage was changed in the range of 0.125 - 0.5 in order to control the copolymer compositions of P(3HB-co-3HV) contained in the cells. After incubated in a rotary shaker (55 rpm) for 96 hours at 30°C, the cells were centrifuged, washed with acetone, and then dried for 20 min at 70°C. The obtained dried powder cells were homogenized using an agate mortar before being subjected to reactive Py-GC and conventional GC involving off-line trans-methylation.

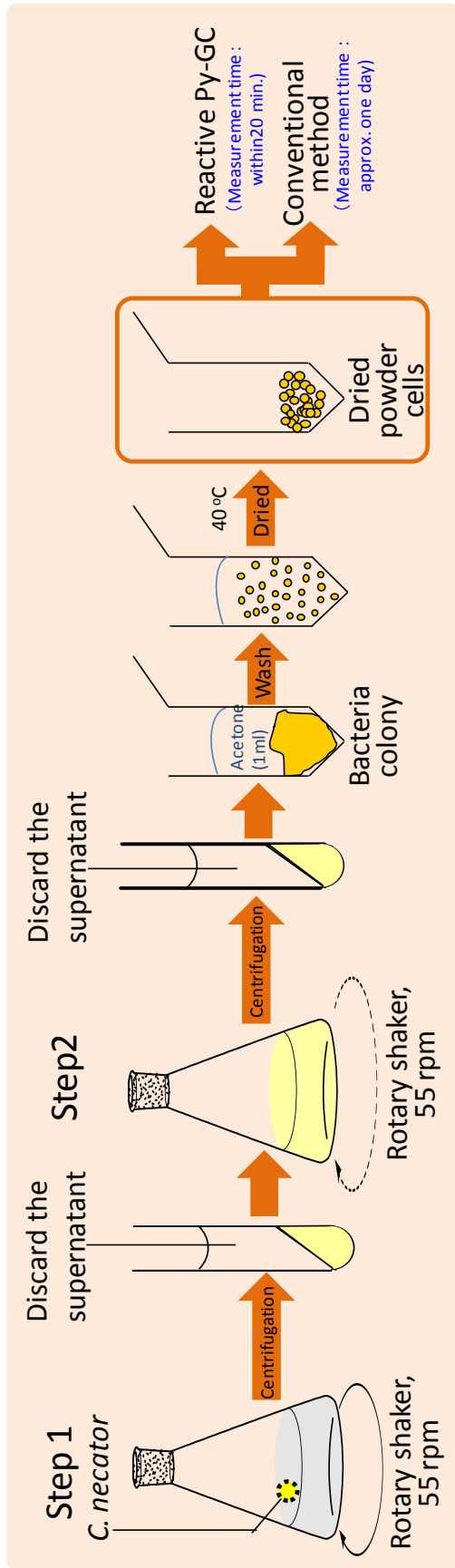


Figure 4.2 : Preparation procedure of dried powder cells containing P(3HB-co-3HV) copolymer.

4.2.3 Reactive Py-GC measurement

The reactive Py-GC system used in this study was basically the same as that described in previous chapter. A vertical microfurnance pyrolyzer (PY-2020iD, Frontier Laboratories, Koriyama, Japan) was attached to a GC (GC2010 Plus, Shimadzu, Kyoto, Japan) equipped with a flame ionization detector (FID). A small platinum samples cup (2 mm i.d. × 4 mm height) containing 30 ± 5 μg of the powder samples of the bacterial cells or P(3HB-*co*-3HV) together with 4 μl of TMAH solution was dropped into the heated center of a pyrolyzer maintained at 400°C under a helium carrier gas flow (50 ml/min). A part of the flow (1 ml/min) reduced by a splitter was introduced into a metal capillary separation column (Ultra ALLOY-5 (MS/HT); 30 m long × 0.25 mm i.d., Frontier Laboratories) coated with immobilized 5% diphenyl-95% dimethylpolysiloxane (1.0 μm film thickness). The column temperature was programmed from 35 to 300°C at a rate of 5°C/min. Identification of the peaks on the chromatograms was carried out by using a reactive Py-GC-mass spectrometer (MS) (QP-5050, Shimadzu) with an electron ionization (EI) source.

4.2.4 Procedure for trans-methylation and solvent extraction followed by GC analysis

Trans-methylation and solvent extraction of P(3HB-*co*-3HV) in the bacterial cells weighing ca. 20 mg were performed according to the procedure reported by Braunegg et al.¹¹ as shown in Figure 4.3. The methyl esters of 3HB and 3HV, prepared through trans-methylation with methanol containing 10% H₂SO₄ at 100°C for 3.5 hours, were extracted with water and then analyzed by an ordinary GC system under the same chromatographic conditions as for the reactive Py-GC measurements.

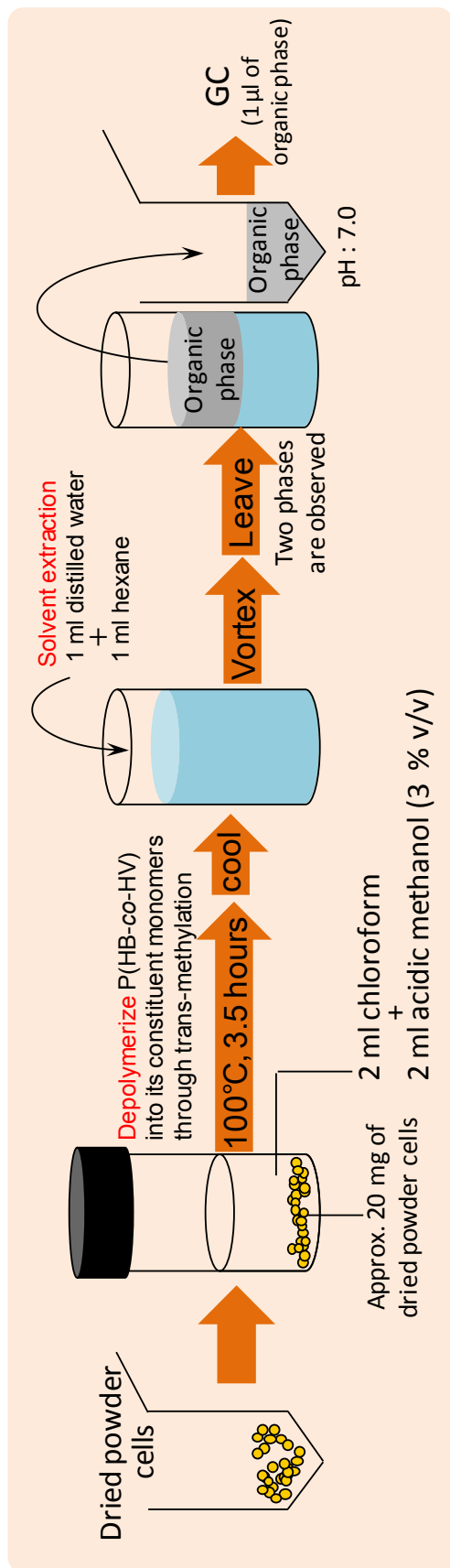


Figure 4.3 : Procedure for conventional method extraction involving off-line trans-methylation and solvent extraction.

4.3 Results and Discussion

Figure 4.4 shows typical pyrograms of (a) industrially available P(3HB-*co*-3HV) and (b) intact *C. necator* cells cultured in the medium, in which the ratio of valeric acid to glucose (V/G) was set at 0.125, obtained by reactive Py-GC in the presence of TMAH at 400°C. As reported by Sato et. al.,¹⁵ on the pyrogram of P(3HB-*co*-3HV) (a), a series of peaks attributed to the products from 3HB unit (peaks 1 - 3, and 8) and 3HV unit (peaks 4 - 7, and 9) were clearly observed after the elution of the reagent-related products. Table 4.1 summarizes the assignment of these characteristic peaks with their molecular structures, origins, and effective carbon numbers (ECN) corresponding to the relative molar sensitivities for FID.¹⁸ Among these products, the peak 8 (methyl 3-methoxybutanoate) and peak 9 (methyl 3-methoxypentanoate) were formed from 3HB and 3HV units, respectively, through the typical pyrolysis reaction. The other products with olefinic structures were considered to be generated by *cis*-elimination reaction of the ester linkages followed by the pyrolysis reaction at the adjacent ester bond.¹⁵ Figure 4.5 shows possible pathways to form methyl butenoates from 3HB units in the polymer chains through reactive pyrolysis as proposed by Sato et al.¹⁵ As shown in this figure, the pyrolysis of 3HB units proceeds by *cis*-elimination reactions of the ester linkages to give a pair of carboxylic acids and olefinic intermediates. The hydrolysis and subsequent methylation of olefinic intermediates leads to the formation of peak 1-3. In a similar manner, 3HV units in the polymer chains undergoes *cis*-elimination followed by reactive pyrolysis to yield peak 4-7.¹⁵

Similar to the case for the P(3HB-*co*-3HV) sample, the pyrogram of the *C. necator* sample (b) clearly showed the nine characteristic peaks derived from 3HB and

3HV units in the polymer chains without any appreciable interference by the bacterial matrix components such as lipids and proteins.

Figure 4.6 shows the pyrograms of the *C. necator* samples cultured in a liquid medium with different V/G ratios; (a) 0.125 (the same pyrogram with that in Figure 4.4 (b)), (b) 0.25 and (c) 0.5. The major nine peaks derived from P(3HB-co-3HV) were commonly observed on the pyrograms. Here it should be noted that the relative intensities of peaks 1-3 and 8, which were attributed to 3HB unit, gradually increased as the valeric acid concentration in the medium increased. This phenomenon might be explained by the toxic behavior of the increased amount of valeric acid to *C. necator*, which leads to the inhibition of biosynthesis of 3HV units and/or the change in the metabolic pathway of the bacteria. As proposed by Sato et. al.,¹⁵ the total molar yields for 3HB unit (Y_{3HB}) and 3HV unit (Y_{3HV}) in the chromatograms are calculated from the intensities of the nine characteristic products as follows:

$$Y_{3HB} = \sum_{i=1-3,8} \frac{I_i}{ECNi} \quad (1)$$

$$Y_{3HV} = \sum_{i=4-7,9} \frac{I_i}{ECNi} \quad (2)$$

where I_i is the peak intensity of peak i in Table 4.1, and $ECNi$ is the corresponding ECN. The mole compositions of 3HB unit, C_{3HB} (mol%), and 3HV unit, C_{3HV} (mol%), in

P(3HB-*co*-3HV) accumulated in the bacterial cells are estimated by the following equations, Eqs. (3) and (4), respectively:

$$C_{3HB} \text{ (mol\%)} = \frac{Y_{3HB}}{Y_{3HB} + Y_{3HV}} \times 100 \quad (3)$$

$$C_{3HV} \text{ (mol\%)} = \frac{Y_{3HV}}{Y_{3HB} + Y_{3HV}} \times 100 \quad (4)$$

Furthermore, to evaluate the accuracy of the reactive Py-GC method, the products from off-line trans-methylation and solvent extraction of the bacterial cells were analyzed by an ordinary GC system. Figure 4.7 shows pyrograms of the solvent extracts from the *C. necator* samples cultured in the medium with different V/G ratios: (a) 0.125, (b) 0.25 and (c) 0.5. After elution of the solvent peaks, the peaks of methyl 3-hydroxybutanoate and methyl 3-hydroxyvalerate, derived from trans-methylation of 3HB and 3HV units, respectively, in the polymer backbones, were unambiguously observed on each pyrogram. In a way similar to the tendency shown in Figure 4.6, the relative intensity of methyl 3-hydroxybutanoate, attributed to 3HB unit, gradually increased with an increase in the valeric acid concentration in the medium. The copolymer compositions of the 3HB unit, C_{3HB} (mol%), and 3HV unit, C_{3HV} (mol%) in P(3HB-*co*-3HV) were calculated from the intensities of these two peaks observed on the pyrograms as follows:

$$C_{3HB} \text{ (mol\%)} = \frac{I_{3HB}/ECN_{3HB}}{I_{3HB}/ECN_{3HB} + I_{3HV}/ECN_{3HV}} \times 100 \quad (5)$$

$$C_{3HV} \text{ (mol\%)} = \frac{I_{3HV}/ECN_{3HV}}{I_{3HB}/ECN_{3HB} + I_{3HV}/ECN_{3HV}} \times 100 \quad (6)$$

where I_{3HB} and I_{3HV} are the peak intensities of methyl 3-hydroxybutanoate and methyl 3-hydroxyvalerate, respectively, and ECN_{3HB} and ECN_{3HV} are their corresponding ECN values (3.0 and 4.0, respectively).

Table 4.2 summarizes the data for the copolymer compositions of P(3HB-*co*-3HV) in the three *C. necator* samples obtained by the reactive Py-GC method with those by the conventional method. As shown in this table, the values obtained by both methods were overall in good agreement for each sample, although a slight discrepancy was observed in a manner that the values for 3HV unit by reactive Py-GC were somewhat lower than those by the conventional method. This observation could be due to the less polarity of the 3HV unit than that of the 3HB unit, which in turn results in a lowered reaction efficiency of 3HV unit with TMAH. Furthermore, the reproducibility for the composition obtained by reactive Py-GC was less than 5% based upon the relative standard deviation (RSD) values for three repeated runs, suggesting satisfactory reproducibility to estimate the composition of P(3HB-*co*-3HV) in bacterial cells directly.

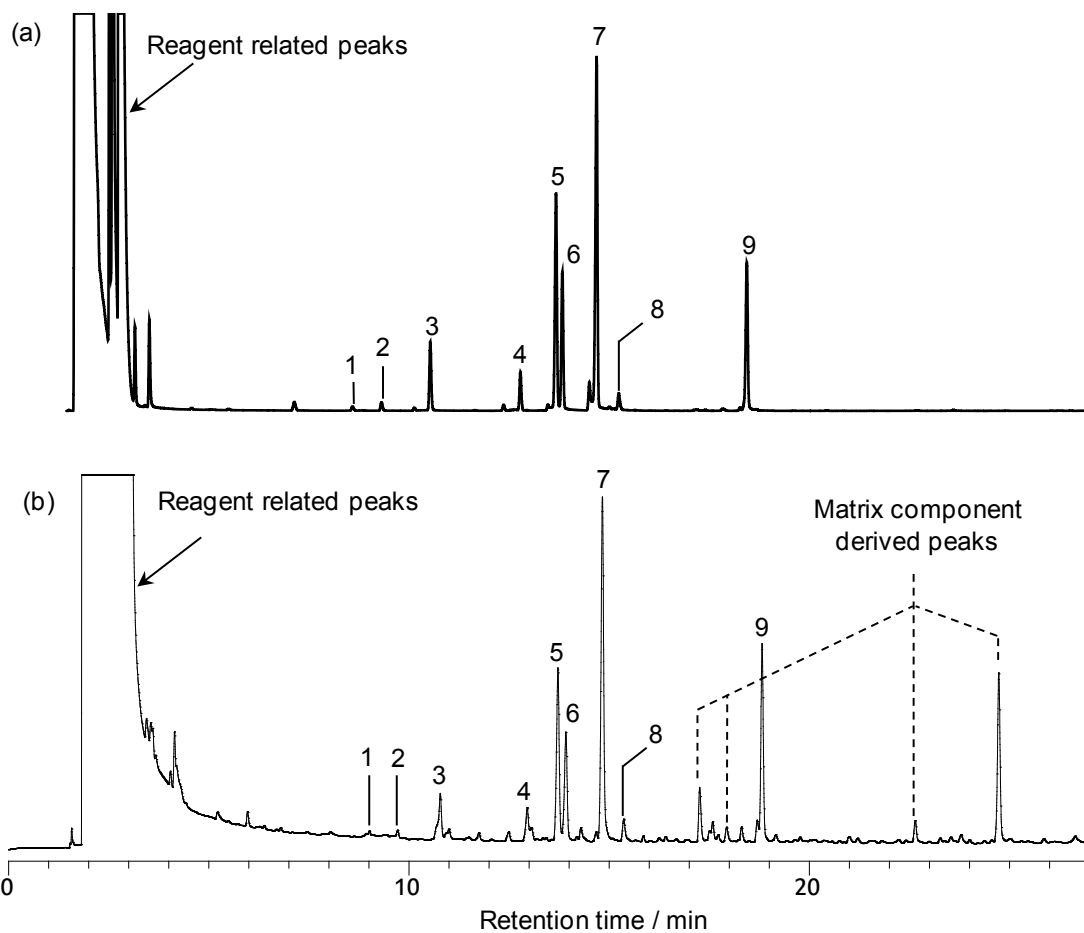
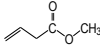
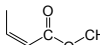
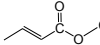
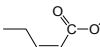
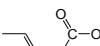
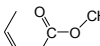
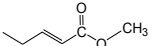
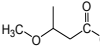
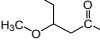


Figure 4.4 : Pyrograms of (a) industrially available P(3HB-*co*-3HV) and (b) intact *C. necator* cells cultured in medium ($V/G = 0.125$) obtained by reactive Py-GC at 400°C. See Table 4.1 for the peak assignment. The identities of labeled peaks are listed in Table 4.1.

Table 4.1 : Identification of the characteristic peaks on pyrograms of Figure 4.4 and 4.6.

Peak number	Compound name	Molecular structure	Origin	ECN ^a
1	Methyl 3-butenolate		3HB	3.65
2	Methyl <i>cis</i> -2-butenolate		3HB	3.65
3	Methyl <i>trans</i> -2-butenolate		3HB	3.65
4	Methyl <i>cis</i> -2-pentenoate		3HV	4.65
5	Methyl <i>trans</i> -3-pentenoate		3HV	4.65
6	Methyl <i>cis</i> -3-pentenoate		3HV	4.65
7	Methyl <i>trans</i> -2-pentenoate		3HV	4.65
8	Methyl 3-methoxybutanoate		3HB	3.95
9	Methyl 3-methoxypentanoate		3HV	4.95

a. Effective carbon number for FID.²⁰

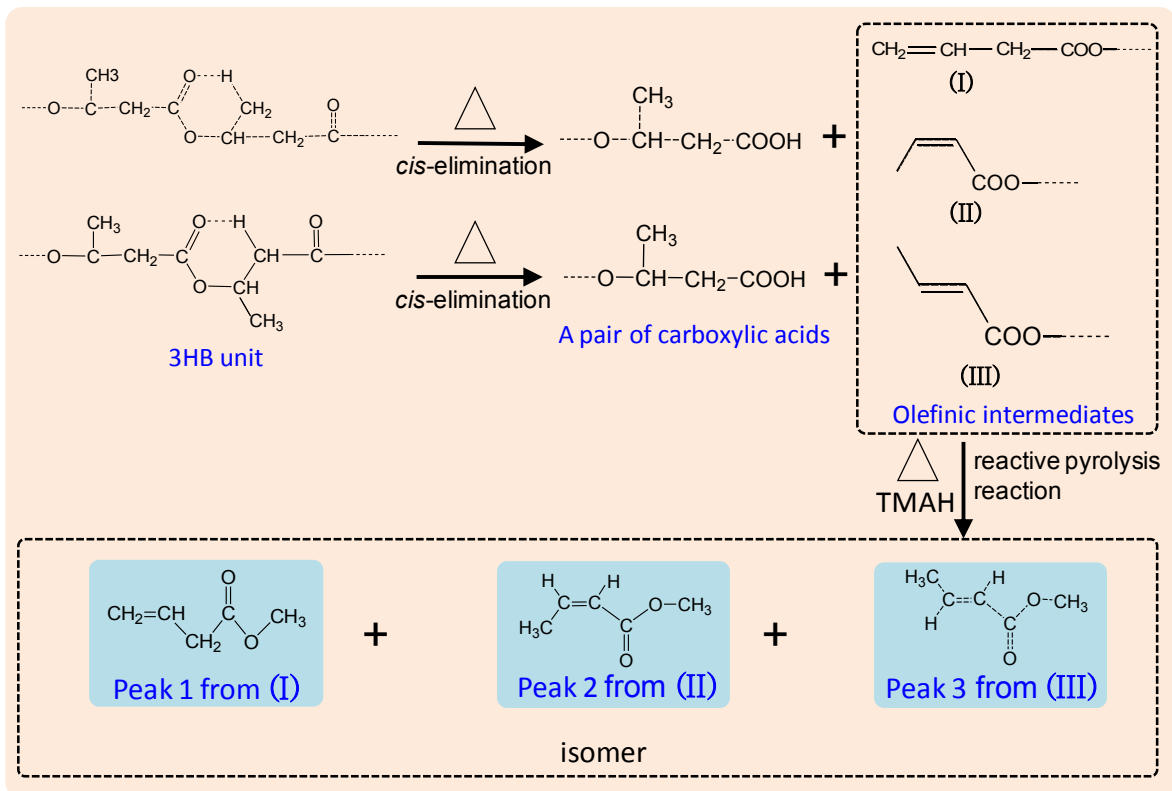


Figure 4.5 : Formation mechanisms of Peak 1-3 through *cis*-elimination reaction followed by reactive pyrolysis reaction.

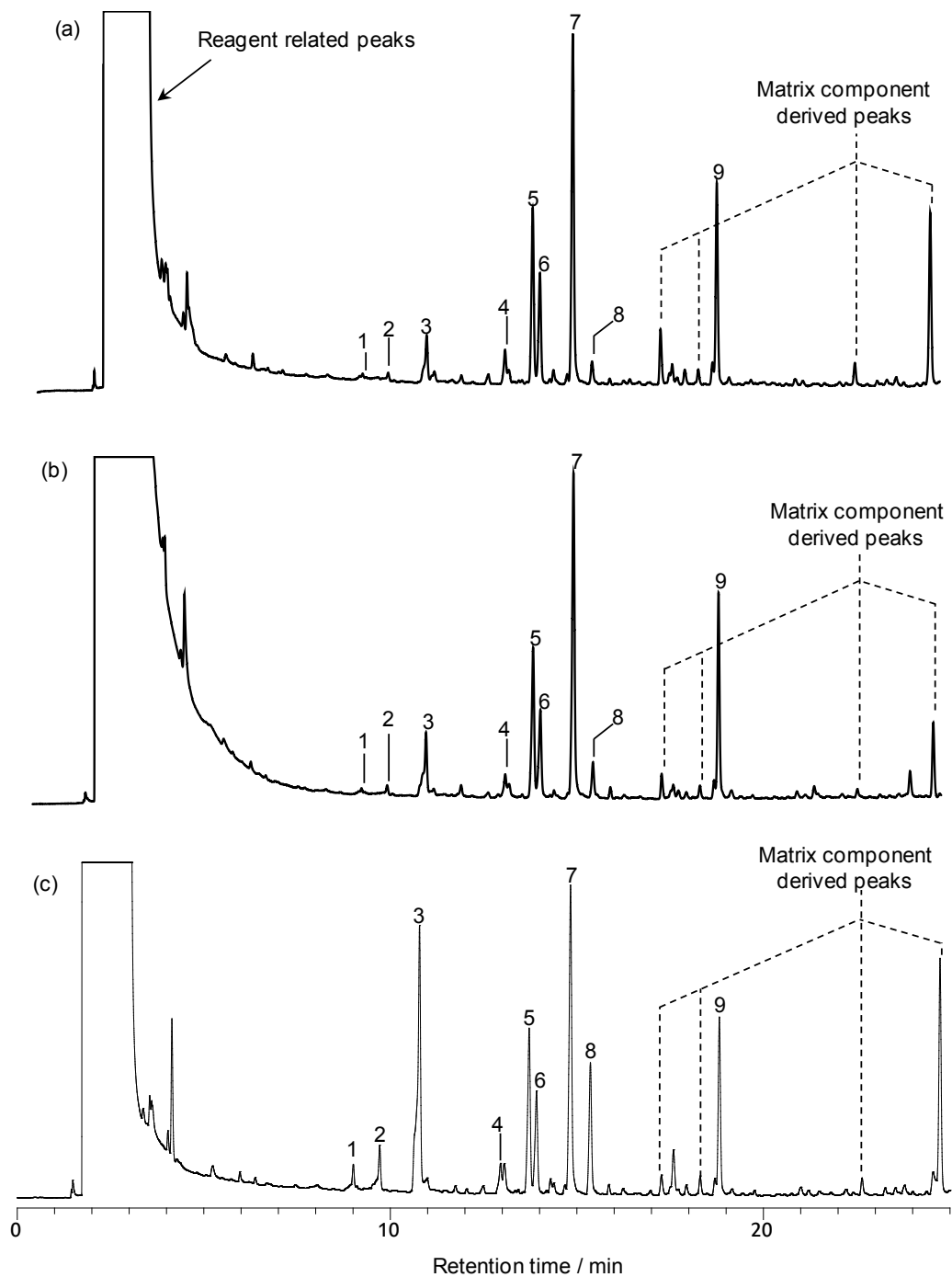


Figure 4.6 : Pyrograms of *C. necator* samples obtained by reactive Py-GC at 400°C. *C. necator* was cultured in liquid medium with different V/G ratios ; (a) 0.125, (b) 0.25, (c) 0.5. See Table 4.1 for the peak assignment. The identities of labeled peaks are listed in Table 4.1.

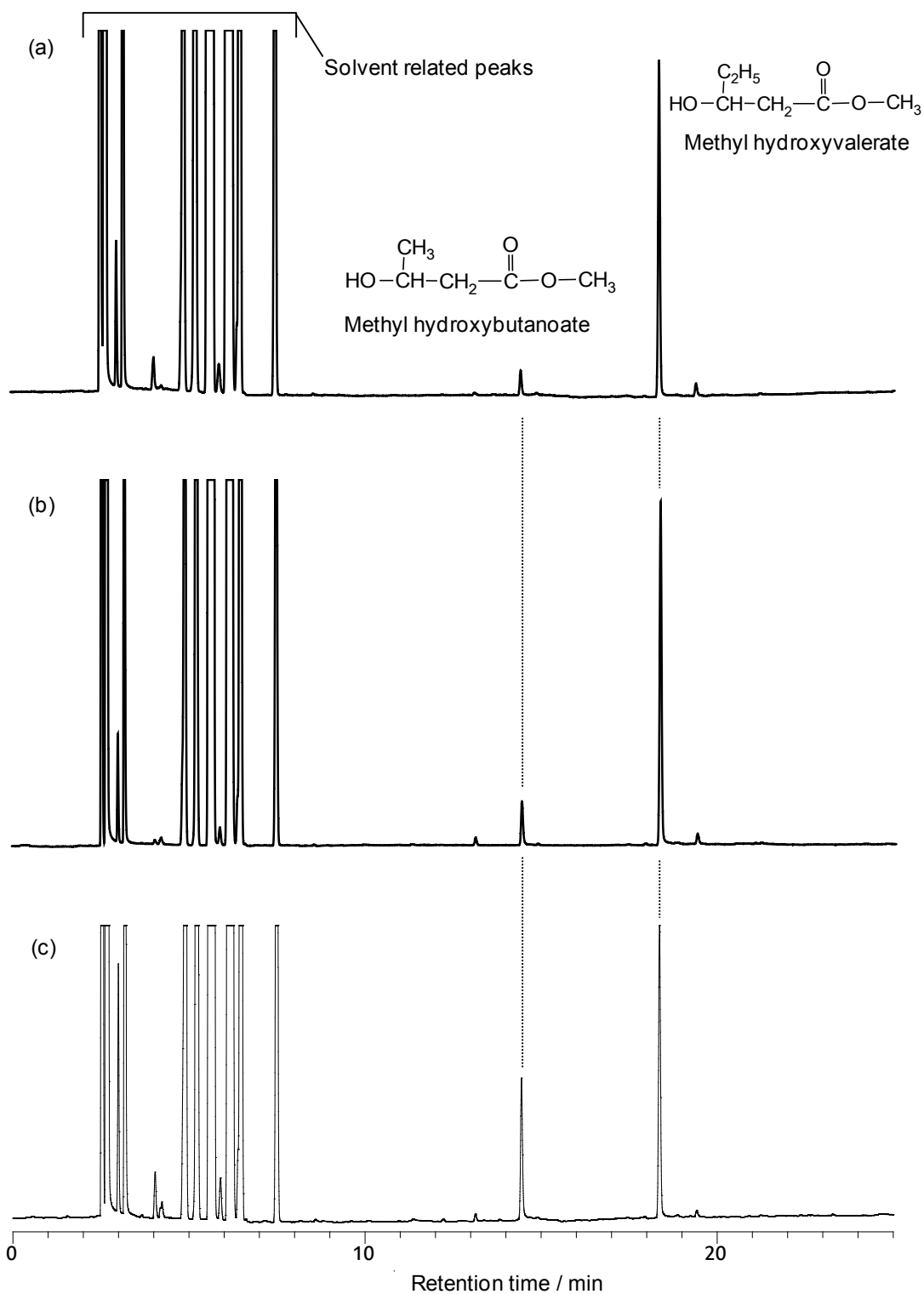


Figure 4.7 : Pyrograms of trans-methylated products of P(3HB-co-3HV) in *C. necator* cells. *C. necator* was cultured in liquid medium with different V/G ratios: (a) 0.125, (b) 0.25, (c) 0.5.

Table 4.2 : Copolymer compositions of P(3HB-*co*-3HV) in *C. necator* obtained by reactive Py-GC and conventional methods.

Molar ratio of valeric acid to glucose (V/G) , %	Composition (3HB : 3HV), mol%	
	Reactive Py-GC	Conventional method
0.125	11.9 : 88.1 (2.4) ^a	9.2 : 90.8 (0.15)
0.25	18.5 : 81.5 (5.0)	14.4 : 85.6 (0.68)
0.50	46.2 : 53.8 (2.9)	43.8 : 56.2 (0.27)

a. Values in parentheses are relative standard deviations ($n = 3$).

4.4 Conclusions

Reactive Py-GC in the presence of TMAH proved to be a rapid and highly sensitive method to determine the copolymer composition of P(3HB-*co*-3HV) accumulated in trace amounts (30 μg) of the *C. necator* cells without using any tedious and/or cumbersome sample pretreatment. This method enabled us to analyze the compositions of P(3HB-*co*-3HV) in whole cells directly with sufficient accuracy and precision. Therefore, this reactive Py-GC method can be used as a practical screening tool for bacteria suited for the production of the copolyester with high performances.

References

1. Y. Proirier, C. Nawrath, and C. Sommerville, *Bio/Technology*, **13**, 142-150 (1995).
2. K. Sudesh, H. Abe, and Y. Doi, *Prog. Polym. Sci.*, **25**, 1503-1555 (2000).
3. Y. Proirer, C. Nawrath, and C. Sommerville, *Nature Biotechnol.*, **13**, 142-150 (1995).
4. M. J. Fabra, G. Sanchez, A. Lopez-Rubio, and J. M. Lagaron, *Food Sci. Technol.*, **59**, 760-767 (2014).
5. T. Ishigaki, W. Sugano, A. Nakanishi, M. Tateda, M. Ike, and M. Fujita, *Chemosphere*, **54**, 225-233 (2004).
6. A. Demirbas, *Energy Sources, Part A*, **29**, 419-424 (2007).
7. Y. Tokiwa, B. P. Calabia, C. W. Ugwu, and S. Aiba, *Int. J. Mol. Sci.*, **10**, 3722-3742 (2009).
8. M. Hakkarainen, *Adv. Polym. Sci.*, **157**, 113-138 (2002).
9. Y. Wang, J. Cai, J. Lan, Z. Liu, N. He, L. Shen, and Q. Li, *Bioresour. Technol.*, **148**, 61-69 (2013).
10. S. O. Kulkarni, P. P. Kanekar, S. S. Nilegaonkar, S. S. Sarnaik, and J. P. Jog, *Bioresour. Technol.*, **101**, 9765-9771 (2010).
11. G. Braunegg, B. Sonnleitner, and R. M. Lafferty, *Eur. J. Appl. Microbiol. Biotechnol.*, **6**, 29-37 (1978).
12. T. Suzuki, T. Yamane, and S. Shimizu, *Appl. Microbiol. Biotechnol.*, **23**, 322-329 (1986).
13. A. Betancourt, A. Yezza, A. Halasz, H. V. Tra, and H. Hawari, *J. Chromatogr. A.*, **1154**, 473-476 (2007).
14. U. Rao, R. Sirdar, and P. K. Segal, *Biochem. Eng. J.*, **49**, 13-20 (2010).

15. H. Sato, M. Hoshino, H. Aoi, T. Seino, Y. Ishida, K. Aoi, and H. Ohtani, *J. Anal. Appl. Pyrolysis*, **74**, 193-199 (2005).
16. S. Chandprateep, Y. Katakura, S. Visetkoop, H. Shimizu, S. Kulpreecha, and S. Shioya, *J. Ind. Microbiol. Biotechnol.*, **35**, 1205-1215 (2008).
17. H. M. Abdelhad, A. M. A. Hafez, A. A. El-Sayed, and T. A. Khodair, *J. Appl. Sci. Res.*, **5**, 343-353 (2009).
18. A. D. Jorgenson, K. C. Picel, and V. C. Stamoudis, *Anal. Chem.*, **62**, 683-689 (1990).

Chapter 5

Conclusion and Future Prospects

The physical properties of biodegradable copolyesters depend not only on their molecular structural features, but also on their chemical compositions. Furthermore, the compositional data of biodegradable copolyesters often provide useful clues for the prediction of biodegradability. These benefits have led to a growing demand for the accurate and precise determination of the compositions of biodegradable copolyesters.

In this study, a practical and highly sensitive method for the determination of the chemical compositions of biodegradable copolyesters using reactive pyrolysis-gas chromatography (reactive Py-GC) in the presence of tetramethylammonium hydroxide (TMAH) was successfully developed.

Chapter 1 outlined the objectives of this study and overviewed current methods for the compositional analysis of biodegradable copolyesters along with the features of reactive Py-GC.

Chapter 2 established a method for the sensitive compositional analysis of poly(butylene succinate-*co*-butylene adipate) [P(BS-*co*-BA)] film samples. By optimizing the pyrolysis temperature, the chemical composition of P(BS-*co*-BA) was determined accurately and precisely using trace amounts (20 μ g) of film samples. Moreover, using the optimized operating conditions, reactive Py-GC was successfully applied to the evaluation of the degree of biodegradation for P(BS-*co*-BA) films after a soil burial degradation test; the relative standard deviation (RSD) was less than 1%.

Chapter 3 clarified in detail the reason for the change in copolymer composition observed for the P(BS-*co*-BA) film samples. To reveal the cause, the biodegradabilities of P(BS-*co*-BA) films with lowered crystallinities were compared with those of the original films using reactive Py-GC. The obtained results led to the following conclusions: (1) the butylene adipate (BA)-rich moieties in the copolymer

chains relatively lower crystallinities than the butylene succinate (BS)-rich moieties; and (2) the BA-rich moieties were preferentially biodegraded during the soil burial test, leading to a decreased BA content as the biodegradation proceeded.

Chapter 4 established a direct and practical method for the compositional analysis of poly(3-hydroxybutyrate-*co*-3-hydroxyvalerate) [P(3HB-*co*-3HV)] accumulated in whole bacteria cells weighing about 30 μg using reactive Py-GC in the presence of TMAH. By using this technique, the chemical composition of P(3HB-*co*-3HV) in bacterial cells was determined with a precision of about 5% of the RSD. Furthermore, the accuracy of the obtained data was also sufficient to use this technique as a tool for the routine analyses of copolyesters in bacteria.

The developed method proved to be a rapid and highly sensitive tool to analyze the chemical composition of various biodegradable copolyesters without the use of any tedious and time-consuming sample pretreatment process. This method is expected to have extensive applications such as the lifetime prediction of biodegradable polyesters and the screening of bacteria suited for the production of the polyesters with high performances.

List of Publication

1. Evaluation of Biodegradability of Poly(butylene succinate-*co*-butylene adipate) on the Basis of Copolymer Composition Determined by Thermally Assisted Hydrolysis and Methylation-Gas Chromatography.
S. Baidurah, S. Takada, K. Shimizu, S. Arimoto, Y. Ishida, T. Yamane, and H. Ohtani.
Int. J. Polym. Anal. Charact., 17, 29-37 (2012).
2. Evaluation of Biodegradation Behavior of Poly(butylene succinate-*co*-butylene adipate) with Lowered Crystallinity by Thermally Assisted Hydrolysis and Methylation-Gas Chromatography.
S. Baidurah, S. Takada, K. Shimizu, Y. Ishida, T. Yamane, and H. Ohtani.
J. Anal. Appl. Pyrolysis, 103, 73-77 (2013).
3. Rapid and Direct Compositional Analysis of Poly(3-hydroxybutyrate-*co*-3-hydroxyvalerate) in Whole Bacterial Cells by Thermally Assisted Hydrolysis and Methylation-Gas Chromatography.
S. Baidurah, Y. Kubo, M. Kuno, K. Koderu, Y. Ishida, T. Yamane, and H. Ohtani.
Anal. Sci., 31, 79-83 (2015).

Acknowledgements

This dissertation would not have been possible without the guidance and the help of several individuals who contributed and extended their valuable assistance in the preparation and completion of this research study.

First, I would like to express my utmost gratitude to my thesis advisor, **Dr. Yasuyuki Ishida**, for providing me with the initial idea, I have needed to do this research. Being the first PhD student under his supervision, I hope that my achievement met his requirements, if not exceeding them.

My deep gratitude goes to **Prof. Tsuneo Yamane**, who even after the event of his retirement, still now offers his concern regarding my research project and journal publications. I also thank **Prof. Shigeru Suzuki** and **Prof. Atsushi Yamamoto**, who contributed much support, knowledge, and useful feedback.

A special word of gratitude is due to **Prof. Hajime Ohtani**, Department of Materials Sciences and Engineering, Graduate School of Engineering, Nagoya Institute of Technology, for his inputs, especially in the methodology and instrumentation as part of this study. My thanks extended to **Dr. Yasuo Takagi**, National Industrial Research Institute of Nagoya, for his helpful advice and discussions concerning DSC measurements.

Many thanks to all the lab members for the year 2010-2015 who have helped me along the way in making this research a success.

Thank you to my English language lecturer, Chubu University Language Center, Division of English Education, Faculty of General Education, **Amy Stotts** for teaching and flawlessly correcting my English grammar.

I am thankful and indebted to my husband, **Engr. Mohd Rahmat**, who has let

me pursue my desire to gain more knowledge. To my dear **Iman Irina**, to whom I can only offer love, and thanks for restraining her hands, lest this dissertation be filled with crayon doodling. A special gratitude to all of my extended family members for their continuing support all these years.

Last, but not least, I am grateful to the one above all of us, the omnipresent God, for giving me the strength to hurdle over all the obstacles in the completion of this research study.